STATE OF THE CALIFORNIA CURRENT 2014–15: IMPACTS OF THE WARM-WATER "BLOB"

ANDREW W. LEISING,
ISAAC D. SCHROEDER,
STEVEN J. BOGRAD

Environmental Research Division
National Marine Fisheries Service
99 Pacific St., Suite 255A
Monterey, CA 93940-7200

JEFFREY ABELL

Department of Oceanography
Humboldt State University

REGINALDO DURAZO[1],
GILBERTO GAXIOLA-CASTRO[2,§]

[1]UABC-Facultad de Ciencias Marinas
Carretera Ensenada-Tijuana No. 3917
Zona Playitas, Ensenada
Baja California, México

[2]CICESE
Departamento de Oceanografía Biológica
Carretera Ensenada Tijuana No. 3918
Zona Playitas, Ensenada
Baja California, México

[§]Monterey Bay Aquarium Research Institute
Moss Landing, California (Sabbatical)

ERIC P. BJORKSTEDT, JOHN FIELD,
KEITH SAKUMA

Fisheries Ecology Division
National Marine Fisheries Service
110 Schaeffer Rd.
Santa Cruz, CA 95060

ROXANNE R. ROBERTSON

CIMEC, Humboldt State University

RALF GOERICKE

Scripps Institute of Oceanography
University of California, San Diego
La Jolla, CA 92024

WILLIAM T. PETERSON,
RICHARD D. BRODEUR

Northwest Fisheries Science Center
National Marine Fisheries Service
Hatfield Marine Science Center
Newport, OR 97365

CAREN BARCELÓ

College of Earth, Ocean and
Atmospheric Sciences
Oregon State University
Corvallis, OR 97330

TOBY D. AUTH[1], ELIZABETH A. DALY[2]

[1]Pacific States Marine Fisheries Commission
Hatfield Marine Science Center
2030 Marine Science Drive
Newport, OR 97365

[2]Cooperative Institute for
Marine Resources Studies
Oregon State University
Hatfield Marine Science Center
2030 Marine Science Drive
Newport, OR 97365

ROBERT M. SURYAN[1],
AMANDA J. GLADICS[1],
JESSICA M. PORQUEZ[2]

[1]Department of Fisheries and Wildlife and
[2]College of Earth, Ocean, and
Atmospheric Sciences
Oregon State University
Hatfield Marine Science Center
Newport, OR 97365

SAM MCCLATCHIE, EDWARD D. WEBER,
WILLIAM WATSON

NMFS
Southwest Fisheries Science Center
8901 La Jolla Shores Drive
La Jolla, CA 92037-1508

JARROD A. SANTORA,
WILLIAM J. SYDEMAN

Farallon Institute for
Advanced Ecosystem Research
101 H Street
Petaluma, CA 94952

SHARON R. MELIN

National Marine Fisheries Service
Alaska Fisheries Science Center
National Marine Mammal Laboratory
NOAA
7600 Sand Point Way N. E.
Seattle, WA 98115

FRANCISCO P. CHAVEZ

Monterey Bay Aquarium Research Institute
7700 Sandholdt Road
Moss Landing, CA 95039

RICHARD T. GOLIGHTLY,
STEPHANIE R. SCHNEIDER

Department of Wildlife
Humboldt State University
1 Harpst Street
Arcata, CA 95521

JENNIFER FISHER,
CHERYL MORGAN

Oregon State University
Cooperative Institute for
Marine Resources Studies
Hatfield Science Center
Newport, OR 97365

RUSSELL BRADLEY,
PETER WARYBOK

Point Blue Conservation Science
3820 Cypress Drive, Suite 11
Petaluma, CA 94954

ABSTRACT

In 2014, the California Current (~28°–48°N) saw average, or below average, coastal upwelling and relatively low productivity in most locations, except from 38°–43°N during June and July. Chlorophyll-*a* levels were low throughout spring and summer at most locations, except in a small region around 39°N. Catches of juvenile rockfish (an indicator of upwelling-related fish species) remained high throughout the area surveyed (32°–43°N). In the fall of 2014, as upwelling ceased, many locations saw an unprecedented increase in sea surface temperatures (anomalies as large as 4°C), particularly at 45°N due to the coastal intrusion of an extremely anomalous pool of warm water. This warm surface anomaly had been building offshore in the Gulf of Alaska since the fall of 2013, and has been referred to as the "blob." Values of the Pacific Decadal Oscillation index (PDO) continued to climb during 2014, indicative of the increase in warm coastal surface waters, whereas the North Pacific Gyre Oscillation index (NPGO) saw a slight rebound to more neutral values (indicative of average productivity levels) during 2014. During spring 2015, the upwelling index was slightly higher than average for locations in the central and northern region, but remained below average at latitudes south of 35°N. Chlorophyll *a* levels were slightly higher than average in ~0.5° latitude patches north of 35°N, whereas productivity and phytoplankton biomass were low south of Pt. Conception. Catches of rockfish remained high along most of the coast, however, market squid remained high only

[1]Details on sampling protocols are available in previous reports and at http://www.nwfsc.noaa.gov/research/divisions/fe/estuarine/oeip/ka-hydrography-zoo-ichthyoplankton.cfm.

within the central coast (36°–38°N), and euphausiid abundance decreased everywhere, as compared to the previous year. Sardine and anchovy were nearly absent from the southern portion of the California Current system (CCS), whereas their larvae were found off the coast of Oregon and Washington during winter for the first time in many years. Waters warmed dramatically in the southern California region due to a change in wind patterns similar to that giving rise to the blob in the broader northeast Pacific. For most of the coast, there were intrusions of species never found before or found at much higher abundances than usual, including fish, crustaceans, tunicates and other gelatinous zooplankton, along with other species often indicative of an El Niño. Thus species richness was high in many areas given the close juxtaposition of coastal upwelling-related species with the offshore warm-water intrusive or El Niño-typical taxa. Thus the California Current by 2015 appears to have transitioned to a very different state than previous observations.

INTRODUCTION

This report reviews the oceanographic and ecosystem responses of the California Current system (CCS) between spring 2014 and summer of 2015. Biological and hydrographic data from a number of academic, private, and government institutions have been consolidated and described in the context of historical data (fig. 1). The various institutions have provided data and interpretations of the data in response to an open solicitation for contributions; these contributions are acknowledged in the author list. These data are summarized and synthesized here, in the spirit of providing a broader description of the present condition of the CCS. All data are distilled from complex sampling programs covering multiple spatial and temporal scales into simple figures that may not convey the full complexity of the region. As a consequence, we focus on the findings of the data and limit our descriptions of the methodology to only that which is required for interpretation. More complete descriptions of the data and methodologies can be found through links to the individual survey programs. The survey designs are dissimilar and each has unique limitations restricting a common interpretation within the CCS. Therefore, this report should be considered a first examination for instigating more focused exploration of potential drivers of the ecosystem dynamics.

This report focuses on data highlighting the conditions during 2014–summer 2015, with a particular emphasis on the conditions associated with several offshore regions of anomalously warm water, the northernmost commonly referred to as the blob (Bond et al. 2015). Similar to last year's report, we have moved some of the physical supporting data from this document to an online supplement (www.calcofi.org/ccpublications/state-of-the-california-current-live-supplement.html). The goal is to create a "live" State of the California Current (SOTCC) web page resource, where information can be rapidly obtained for the most recent, up-to-date state of the CCS. Thus, several long-term time series of physical and biological data that have traditionally been found within this document have been replaced by a table stating only their current state, along with a link to the appropriate web page. As in past reports, we begin with an analysis of large-scale climate modes and upwelling conditions in the California Current. Following, the various observational data sampling programs are reviewed to highlight the links between ecosystem structure, processes, and climate. Lastly, a short discussion of the most recent conditions within the CCS and the impacts of the blob are discussed.

TABLE 1

List of CCS indices, their current status, and link to live supplement (e.g., S1 = Supplement Figure 1; www.calcofi.org/ccpublications/state-of-the-california-current-live-supplement.html).

Index	Current State	Trend	Implication	Link
PDO	Positive	Increasing	Warming	S1
NPGO	Negative	Decreasing	Low Productivity	S1
ENSO (MEI)	Positive	Increasing	El Niño	S1
Upwelling Anomaly	Positive	Neutral	Moderately Productive in the North	Figure 2, S2
Cumulative Upwelling	Neutral	Neutral	Moderately Productive to the North	Figure 3, S3
SST Anomaly	Positive	Increasing	Warm Surface Waters	Figure 4,7, S4, S5, 40
Wind Anomaly	Anti-Cyclonic	Increasing Anti-Cyclonic	Warm Coastal Surface Waters	Figure 4, S4
Temperature-Salinity, CalCOFI	Warmer and Saltier at N Coastal, Surface	NA	Change in Transport	S7
Mixed-Layer Salinity, CalCOFI	Positive Anomaly	Decreasing	NA	Figure 11
Mixed-Layer NO_3, CalCOFI	Negative Anomaly	Neutral	Decreased Productivity	Figure 12
Nitricline Depth, CalCOFI	Negative Anomaly	Decreasing	Decreased Productivity	Figure 12
Integrated Chlorophyll *a*, CalCOFI	Negative Anomaly	Increasing	Decreased Productivity	Figure 12
Chlorophyll *a* Profiles, CalCOFI	Low in Surface waters	NA	Decreased Productivity	S8
Chlorophyll *a*	Patchy	Increasing	Low to Mean Productivity	Figure 5

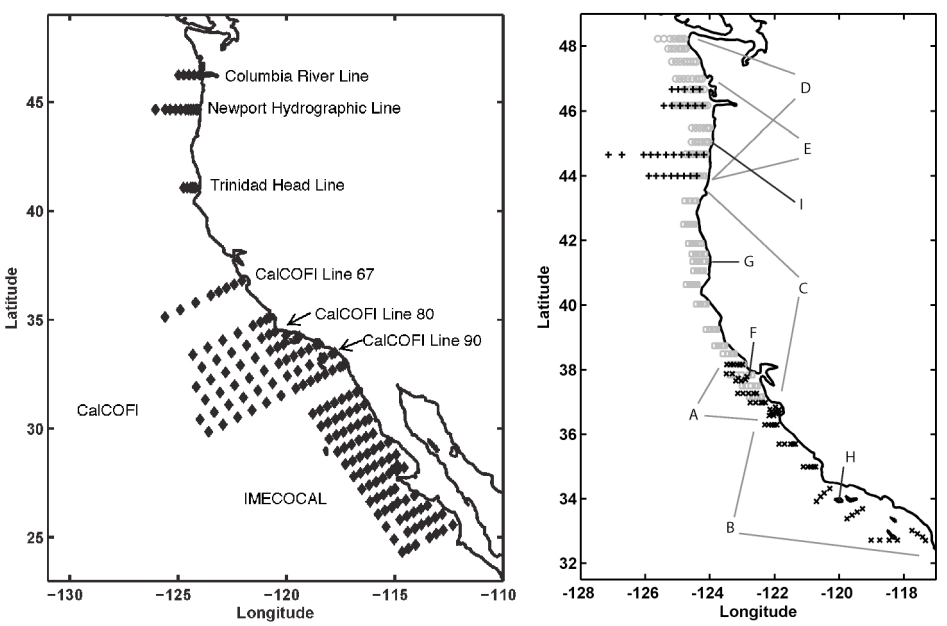

Figure 1. Left: Station maps for surveys that were conducted multiple times per year during different seasons to provide year-round observations in the Califor¬nia Current system. The CalCOFI survey (including CalCOFI Line 67) was occupied quarterly; the spring CalCOFI survey grid extends just north of San Francisco. The IMECOCAL survey is conducted quarterly or semiannually. The Newport Hydrographic Line was occupied biweekly. The Trinidad Head Line was occupied at biweekly to monthly intervals. Right: Location of annual or seasonal surveys, including locations of studies on higher trophic levels, from which data was included in this report. Different symbols are used to help differentiate the extent of overlapping surveys. A. SWFSC Fisheries Ecology Division (FED) midwater trawl survey core region (May–June) B. SWFSC FED midwater trawl survey south region (May–June). C. SWFSC FED salmon survey (June and September) (grey squares). D. NWFSC salmon survey (May, June, and September). E. NOAA/BPA pelagic rope trawl survey (May through September). F. Southeast Farallon Island. G. Castle Rock. H. San Miguel Island. I. Yaquina Head Outstanding Natural Area.

NORTH PACIFIC CLIMATE INDICES

The warm phase in the North Pacific that started in the beginning of 2014 continued through the summer of 2015 (Supplemental fig. S1). The Pacific Decadal Oscillation index (PDO; Mantua et al. 1997) experienced the highest positive value in December 2014 since June 1997. From January 2014 to June 2015 the PDO values were positive—the longest sustained period of positive values since the summer of 2002. The positive values of the PDO can be attributed to the excessively warm sea surface temperature (SST) anomalies experienced first in the northeast Pacific in winter of 2013, which then expanded along the west coast of North America to Baja California, Mexico, during 2014 and 2015 (Bond et al. 2015). The North Pacific Gyre Oscillation (NPGO; Di Lorenzo et al. 2008) index was positive from April 2007 through October 2013, indicating strong circulation in the North Pacific Subtropical Gyre. At the end of 2013 the NPGO switched from the positive values experienced over the previous seven years to negative values. Except for small positive NPGO values in May, October, and November of 2014, the NPGO has remained in a negative state through the summer of 2015. As of June 2015 the multivariate El Niño Southern Oscillation (ENSO) index (MEI; Wolter and Timlin 1998) reached the largest positive value since the strong 1996–98 El Niño. Large positive values of the MEI indicate an El Niño event and NOAA's Climate Prediction Center (http://www.cpc.ncep.noaa.gov) advises that the current El Niño will continue into the winter of 2016.

Upwelling in the California Current

Monthly means of the daily upwelling index (Bakun 1973; Schwing et al. 1996) indicated strong upwelling for the entire year of 2013 especially north of 36°N (fig. 2). Upwelling in 2014 was near the long-term mean for all latitudes, except for a pulse of strong upwelling in June for latitudes between 36° and 42°N. The normal downwelling conditions that occur during the winter at the northern latitudes were reduced in January 2015 due to increased upwelling winds between 33° and 39°N (figs. 3, 4, and S5). For the rest of 2015 upwelling was slightly above the long-term mean for latitudes north of 33°N.

The cumulative upwelling index (CUI) is the cumulative sum of the daily upwelling index starting January 1 and ending on December 31. The CUI provides an estimate of the net influence of upwelling on ecosystem structure and productivity over the course of the year (Bograd et al. 2009). The highest values of

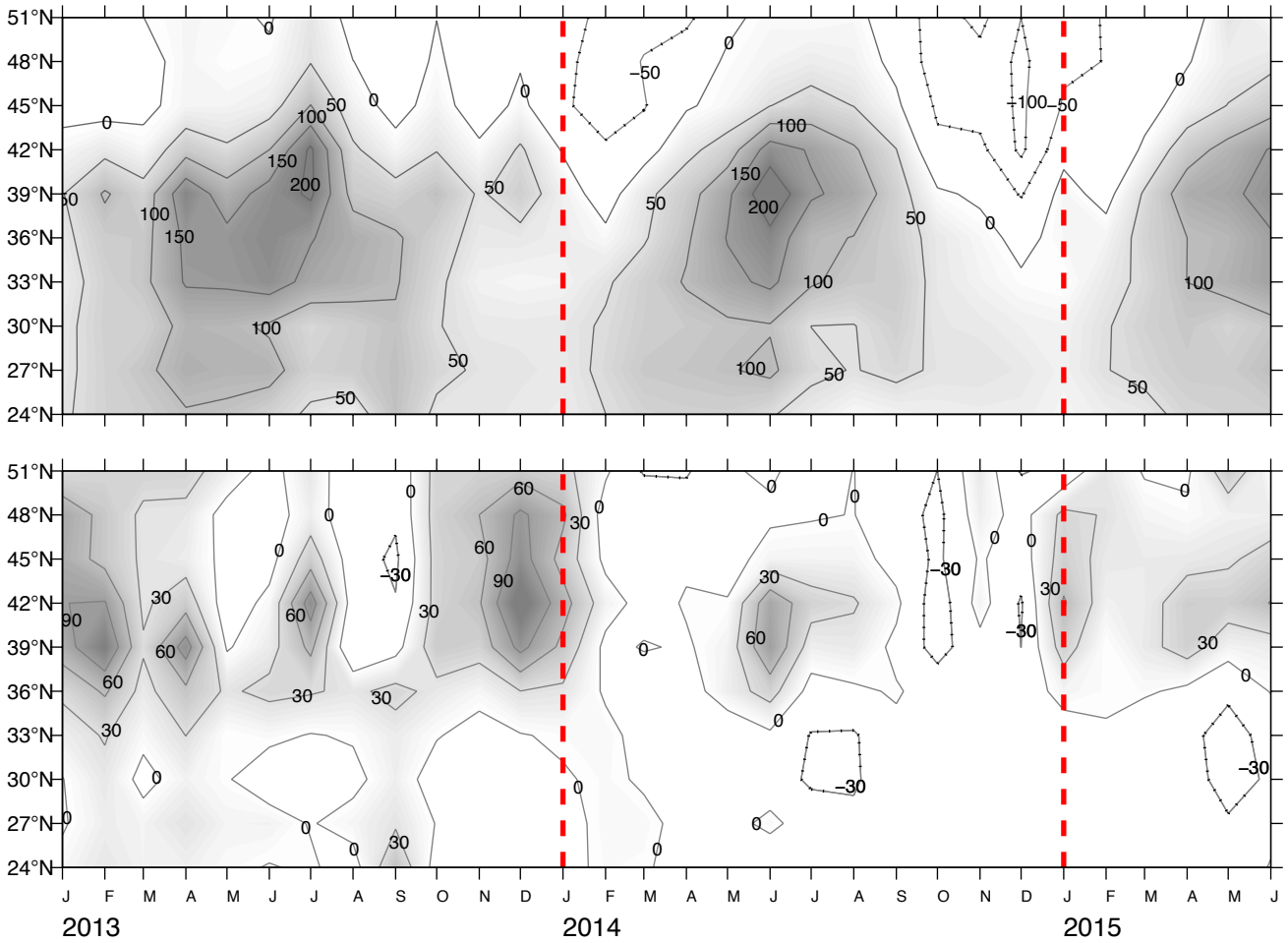

Figure 2. Monthly means of daily Bakun Upwelling Index (top) and anomalies (bottom) for January 2012–July 2015. Shaded areas denote positive (upwelling-favorable) values in upper panel, and positive anomalies (generally greater than normal upwelling) in lower panel. Anomalies are relative to 1967–2014 monthly means. Units are in $m^3\ s^{-1}$ per 100 km of coastline. Daily upwelling index data obtained from http://pfeg.noaa.gov/products/PFELData/upwell/daily.

the CUI for the entire record (1967–2015) occurred in 2013 for latitudes north of 39°N. Upwelling during 2014 was near the long-term mean for the first half of the year (fig. 3). However, after June the CUI from 39 to 44°N was higher than the long-term mean, but south of 33°N the CUI was lower than the long-term mean. Through June 2015, the CUI has been near the long-term average for all latitudes except those between 42° and 48°N. Upwelling winds for these latitudes increased and remained high starting at the beginning of February. Defining the spring transition as the date of the minimum CUI value in the first 151 days of the year it is evident from the strong upwelling in the late winter and early spring that the spring transition date occurred earlier in the year for locations in the north. For example, the spring transition at 42°N was 32 days earlier than the climatological spring transition date of March 16.

North Pacific Climate Patterns

Basin-scale examinations of SST and surface wind vectors allow for the interpretation of the spatial evolution of climate patterns and wind forcing over the North Pacific related to trends in the basin-scale and upwelling indices (fig. S1 and fig. 4). SST anomaly values during July and December of 2014 were generally positive with the largest positive anomalies occurring in the Bering Sea, Gulf of Alaska, and along the west coast of North America down to Baja Mexico. This broad region of persistently high SST anomalies has been termed the blob (Bond et al. 2015), and has been associated with observations of unusual species distributions (described in the Regional Ecosystem Indicators section). The largest positive SST anomalies (over 4.5°C) were located at the entrance of the Gulf of California during July 2014. During the summer and fall of 2014 negative SST anomalies occurred in the region of the Subarctic Frontal Zone, with values lower than –2.5°C during July 2014. A cyclonic wind anomaly was associated with this region of negative SST values. Positive SST anomalies persisted into 2015 with large positive anomalies in the same locations as those in 2014, with the exclusion of the Bering Sea where the anoma-

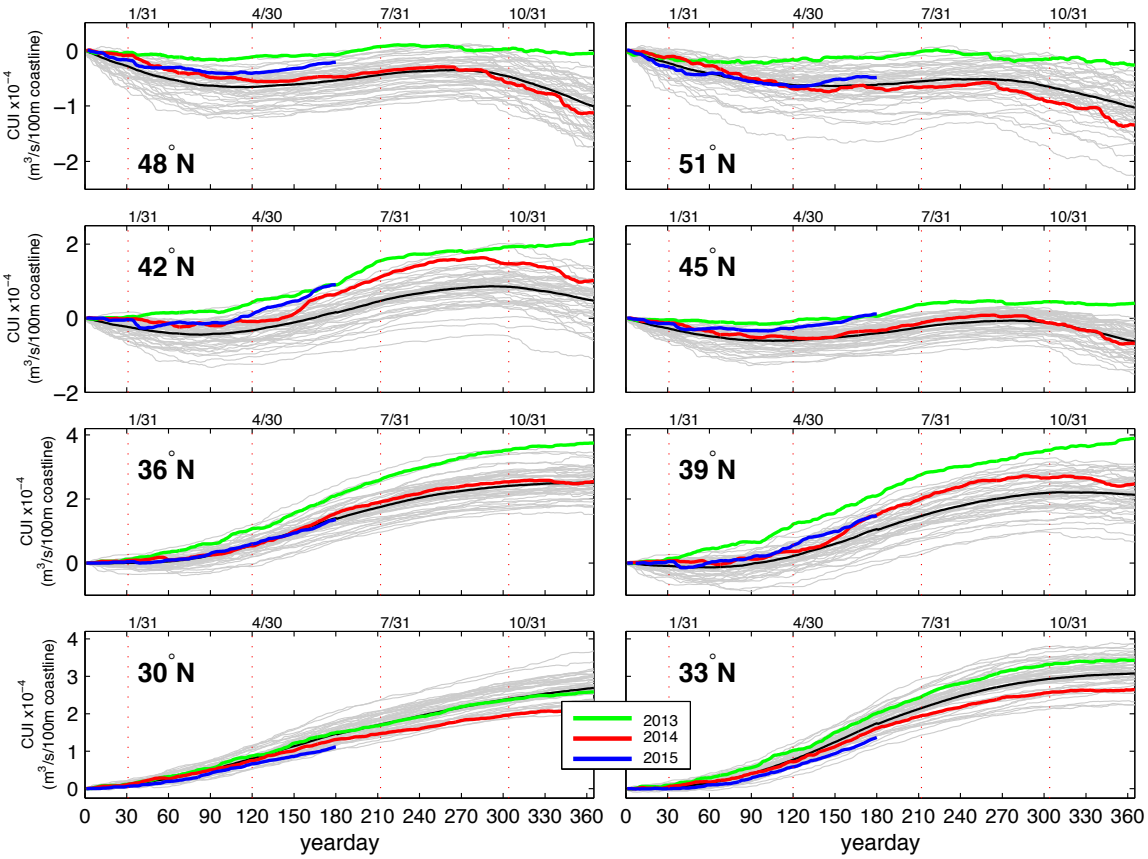

Figure 3. Cumulative upwelling index (CUI) from January 1 calculated from the daily Bakun Upwelling Index at locations along the West Coast of North America for 1967–2013 (grey lines), the mean value for the period 1967–2011 (black line), 2013 (green line), 2014 (red line), and 2015 (blue line). The red dashed vertical lines mark the end of January, April, July, and October.

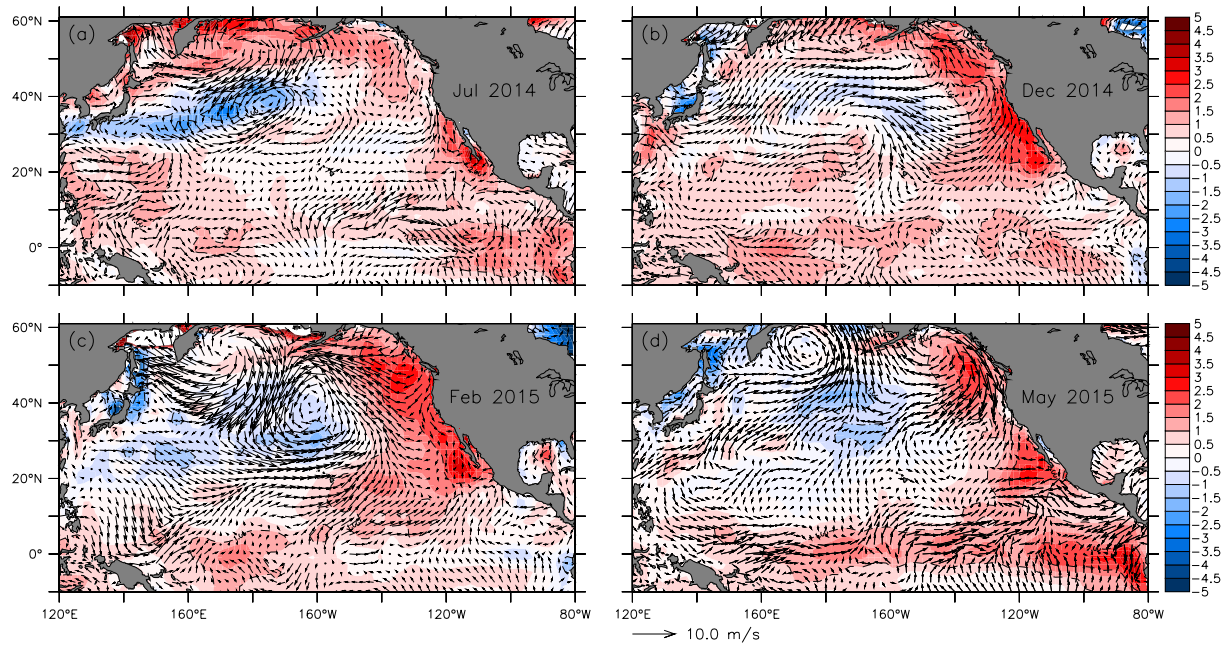

Figure 4. Anomalies of surface wind velocity and sea surface temperature (SST) in the North Pacific Ocean, July 2014, December 2014, February 2015, and May 2015. Arrows denote magnitude and direction of wind anomaly (scale arrow at bottom). Contours demote SST anomaly. Shading interval is 0.5°C and contour intervals of ±1 and 2°C are shown. Negative (cool) SST anomalies are shaded blue. Wind climatology period is 1968–96. SST climatology period is 1950–79. Both SST and wind data are from NCEP/NCAR Reanalysis and were obtained from http://www.esrl.noaa.gov.

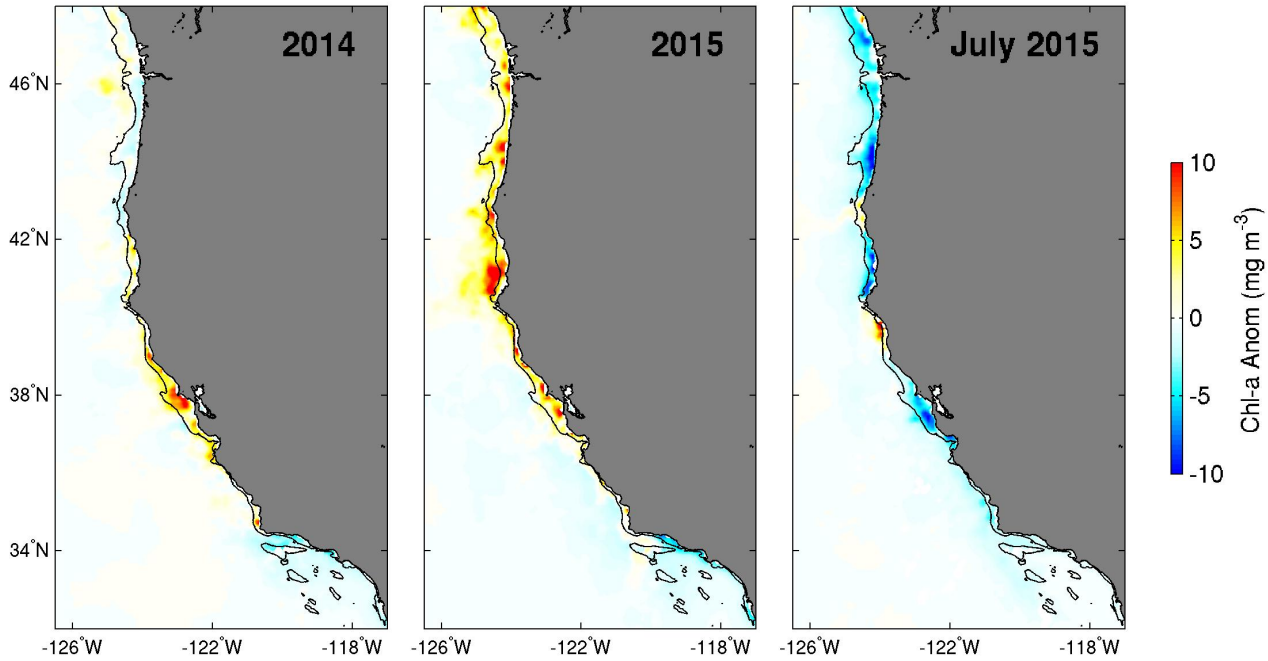

Figure 5. Chlorophyll *a* anomalies from Aqua MODIS for: spring (March–May) of 2014 (left panel), spring (March–May) of 2015 (center), and July 2015 (right panel). Monthly anomalies were averaged onto a 0.1° x 0.1° grid and the climatology was based on the time period from 2002-15. The data were obtained from http://coastwatch.pfel.noaa.gov/.

lies were considerably cooler, but still positive, by May 2015. While the SST anomalies throughout the CCS were extremely warm, the upwelling-favorable alongshore winds in the winter and spring of 2015 were unusually strong (fig. S5). In May 2015 these wind anomalies were the strongest in the north around Washington and Oregon, but the winds lessened in central and southern California. The wind anomalies in the western and central equatorial Pacific indicate strong winds blowing from the west to the east, which might be an indication of westerly wind bursts that could strengthen the current El Niño conditions (Hu et al. 2014).

Coastal Sea Surface Temperature

Daily SST as measured by National Data Buoy Center (NDBC) buoys showed unusually warm SST values from August 2014 to June 2015 for locations throughout the CCS (fig. S5 and fig. 40). The highest deviations from the climatological cycle happened in the late summer and fall of 2014, with some days having temperatures more than 4°C above the long-term mean. Starting in the spring of 2015 the SST values "cooled," but they were still greater than the climatological mean with only a slight drop below for locations between Bodega Bay and Stonewall Bank. The meridional winds during the warm SST period were not unusually weak in magnitude or overly downwelling producing (+ values). The decrease in SST values seen in the central CCS during the spring of 2015 corresponded with an extended period of upwelling producing winds (– values).

Sea Surface Chlorophyll *a*

During spring 2015, sea surface chlorophyll *a* levels, as measured by remote sensing, were higher than average for most of the CCS, excluding the Southern California Bight (fig. 5), likely as a result of the favorable upwelling during this period as compared to the previous year. By summer 2015, sea surface chlorophyll *a* levels were anomalously low in most places, except for a few small patches along the central coast (centered near 38° and 42°N; fig. 5), again reflecting the patterns seen in upwelling across the region.

REGIONAL ECOSYSTEM INDICATORS

Northern California Current: Oregon (Newport Hydrographic Line[1])

The winter of December 2013–March 2014 was quite mild with no large southwesterly storms, resulting in a lack of deep mixing. Bottom waters at midshelf (station NH-5) were colder than normal (fig. 6; second coldest December since the start of the time series in 1997). Beginning in spring of 2014, waters over the Oregon shelf were unusually warm and fresh, with temperatures comparable to those observed during the 1998 El Niño coupled with salinities comparable to those observed in 2003 (fig. 6).

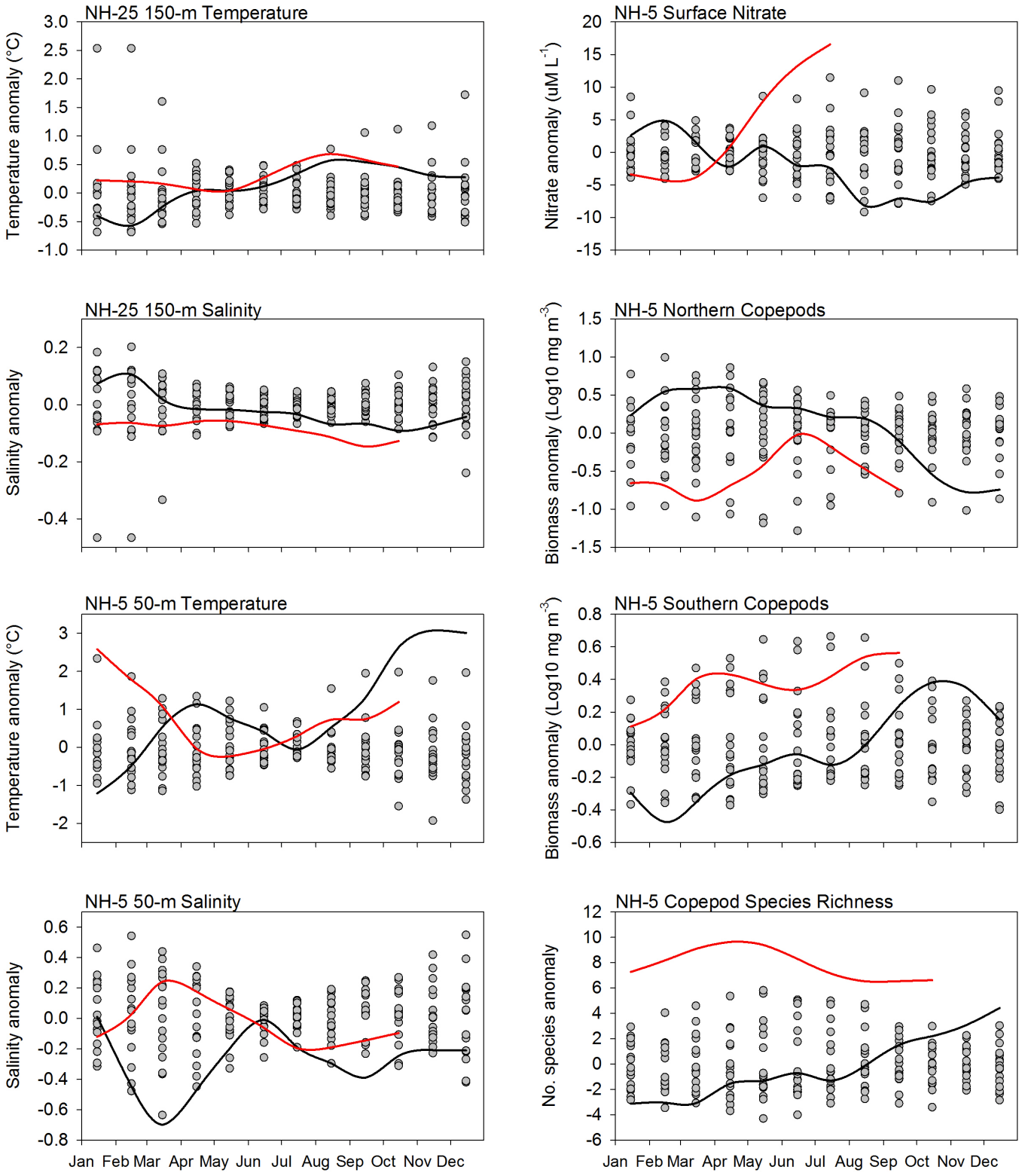

Figure 6. Time-series biophysical plots (Red line = 2015, Black line = 2014, dots = pervious years). Time series plots of local physical and biological anomalies from 1997–present at NH-25 (Latitude: 44.6517°N Longitude: 124.65°W) NH-5 (Latitude: 44.6517°N Longitude: 124.1770°W) along the Newport Hydrographic Line. Temperature and salinity from 150 m and 50 at NH-25 and NH-5 respectively, NO_2 + NO_3 from the surface, and copepod biomass and species richness anomalies are integrated over the upper 60 m. All data were smoothed with a 3-month running mean to remove high frequency variability.

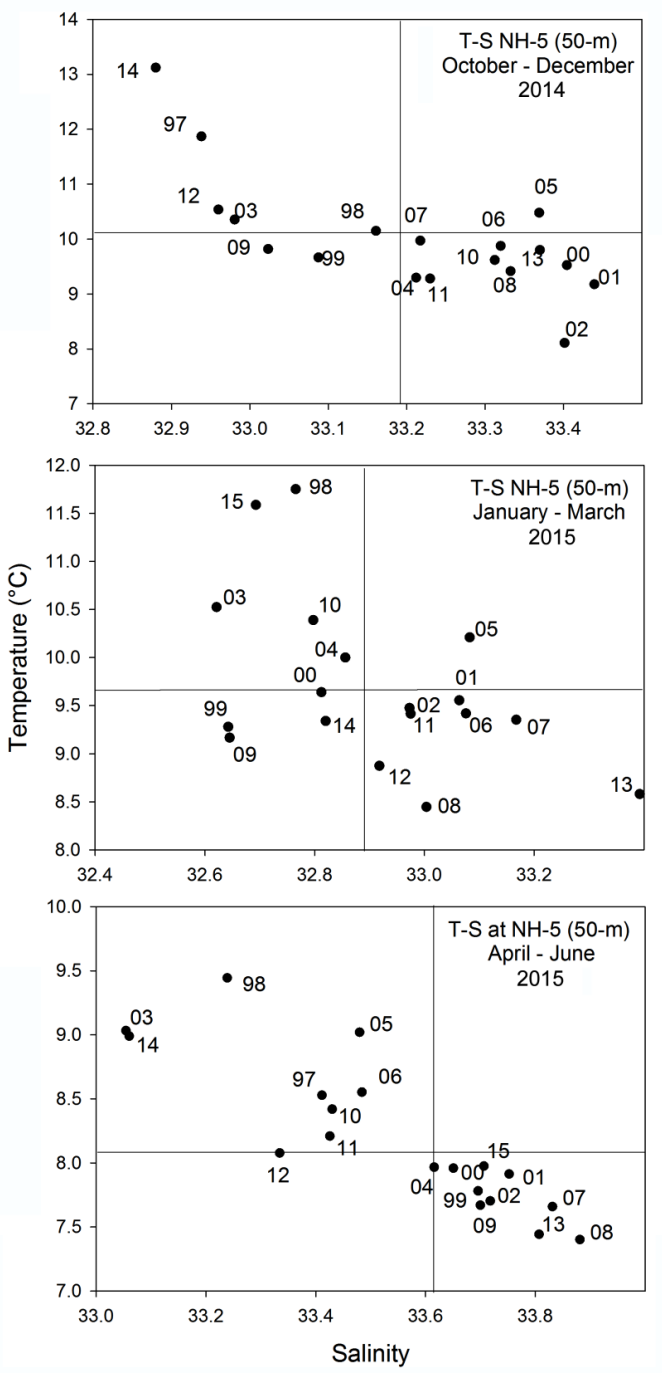

Figure 7. Seasonal mean temperature and salinity at 50 m depth at station NH-5 (Latitude: 44.6517°N Longitude: 124.1770°W) along the Newport Hydrographic Line for October through December 2014 (top panel), January through March 2015 (middle panel), and April through June (bottom panel). Note changes in scale on both temperature and salinity axes. Numbers next to points indicate year of observations.

Upwelling off Oregon was delayed in 2014 (spring transition per CUI on 10 May, or 26 days later than average), and ended 3 weeks earlier than average (20 September 2014), yet total upwelling during this shortened season was near average. As upwelling declined, unusually warm offshore waters rapidly arrived on the shelf, marked by a dramatic increase in SST (peak at 19.4°C, or 4.5°C above normal on 14 September at NDBC Buoy 46050; see fig. 40 for extended history at this location). These waters were warm, fresh, and nutrient-poor (figs. 6 and 7). Deep (50 m) waters on the shelf during the fall and into the winter (October through December, 2014) were the warmest and freshest observed over the past 20 years (comparable to the 1997–98 El Niño), yet deep (150-m) water on the slope during this period was only slightly warmer and fresher than average (fig. 7). This differs substantially from conditions during the 1997–98 El Niño when deep water on the shelf and slope was very warm and fresh (fig. 7).

During spring and summer of 2014, the biomass of northern copepods was moderately high and the biomass of southern copepods and the copepod species richness were relatively low (fig. 6). With the arrival of warm blob waters in late September, the copepod community immediately changed from a lipid-rich "cold water-/upwelling" assemblage to a lipid-poor "warm-water" assemblage, with concomitant decreases in the biomass of northern copepods and increases in the biomass of southern copepods and species richness. Copepod biomass anomalies are comparable to those observed during the 1997–98 El Niño, despite the stronger temperature and salinity anomalies observed in 2014–15. Copepod species richness, however, was the highest observed in the 20-year time series, far exceeding the number of species observed during the strong El Niño event in 1997–98. This increase in species richness reflects the occurrence of at least 17 copepod species that have not previously been (or only rarely) observed in the northern California Current, which is consistent with an unusual and distant source for the waters that arrived in late 2014.

Trinidad Head Line, Northern California

Conditions off northern California in early 2014 reflected a winter marked by weak but consistent northerly winds and relatively mild storm activity, followed by a transition to more intense upwelling-favorable winds that triggered a substantial (>10 μg chlorophyll *a* L^{-1}) phytoplankton bloom over the shelf in late spring to midsummer, peaking in June (fig. 8). Throughout much of 2014, bottom waters on the shelf were warm relative to conditions typically observed at a given time of year. By late summer and early fall, however, midshelf bottom waters were consistently warmer, fresher, and more oxygenated than had been previously reported. A second phytoplankton bloom was observed during late summer and early fall (September), as upwelling winds weakened and became more variable, and stratification increased over the shelf. The arrival of blob waters in the fall followed a transition to increasingly frequent southerly wind events and was marked by strong warm-

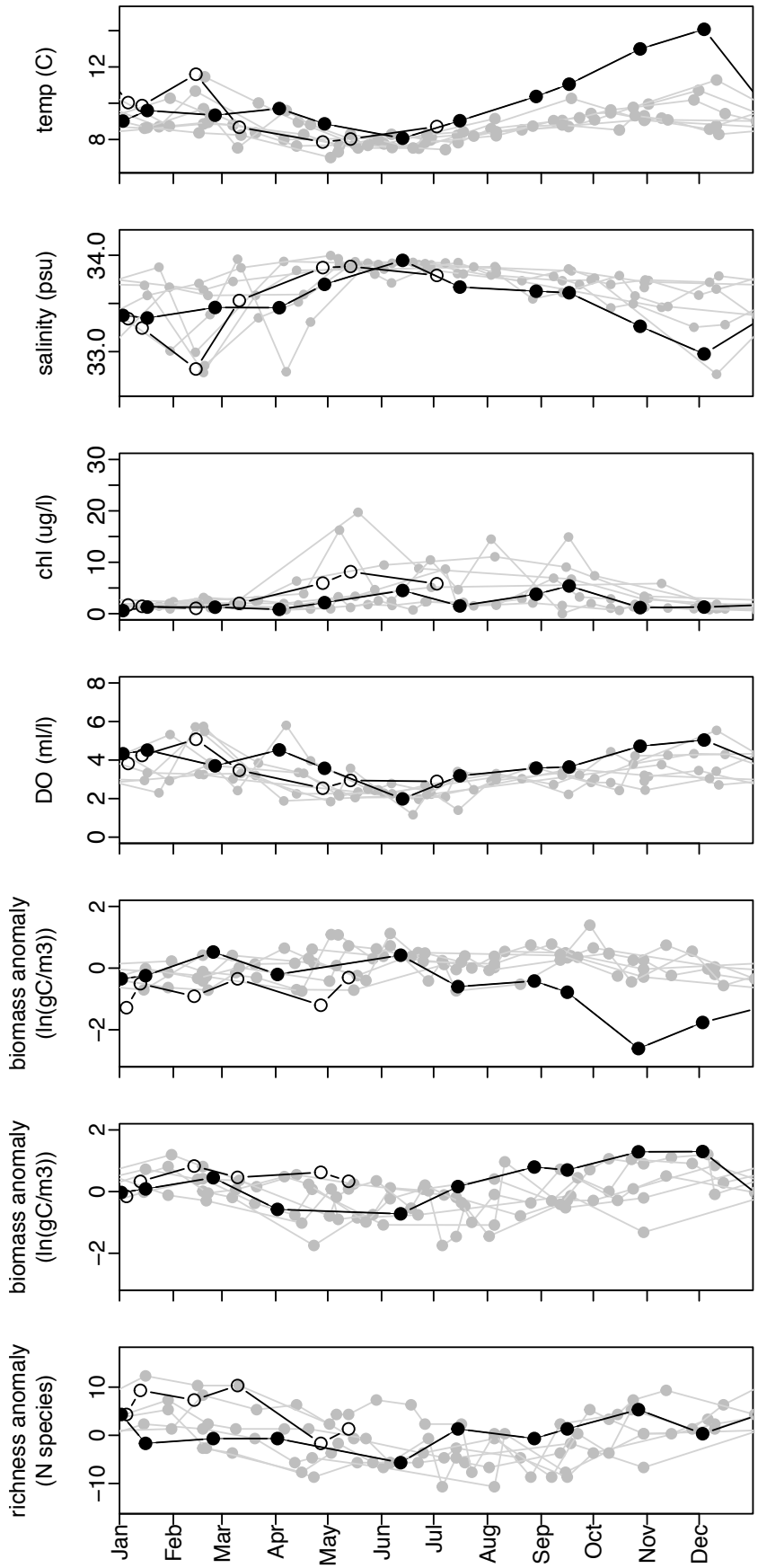

Figure 8. Hydrographic and ecosystem indicators at mid-shelf along the Trinidad Head Line (station TH02; 41°03.5'N, 124°16'W, 75 m depth). Panels from top to bottom show near-bottom (68 m) temperature, near-bottom (68 m) salinity, mean chlorophyll *a* concentration over the upper 30 meters of the water column, near-bottom (68 m) dissolved oxygen concentrations, biomass anomalies for northern copepod species, biomass anomalies for southern copepod species, and species richness anomalies. All assemblages are defined following Hooff and Peterson (2006), and all anomalies are calculated using means from the full time series (2006–15). For all plots, grey symbols indicate historical observations (2006–13), filled circles indicate observations during 2014, and unfilled symbols indicate observations in 2015.

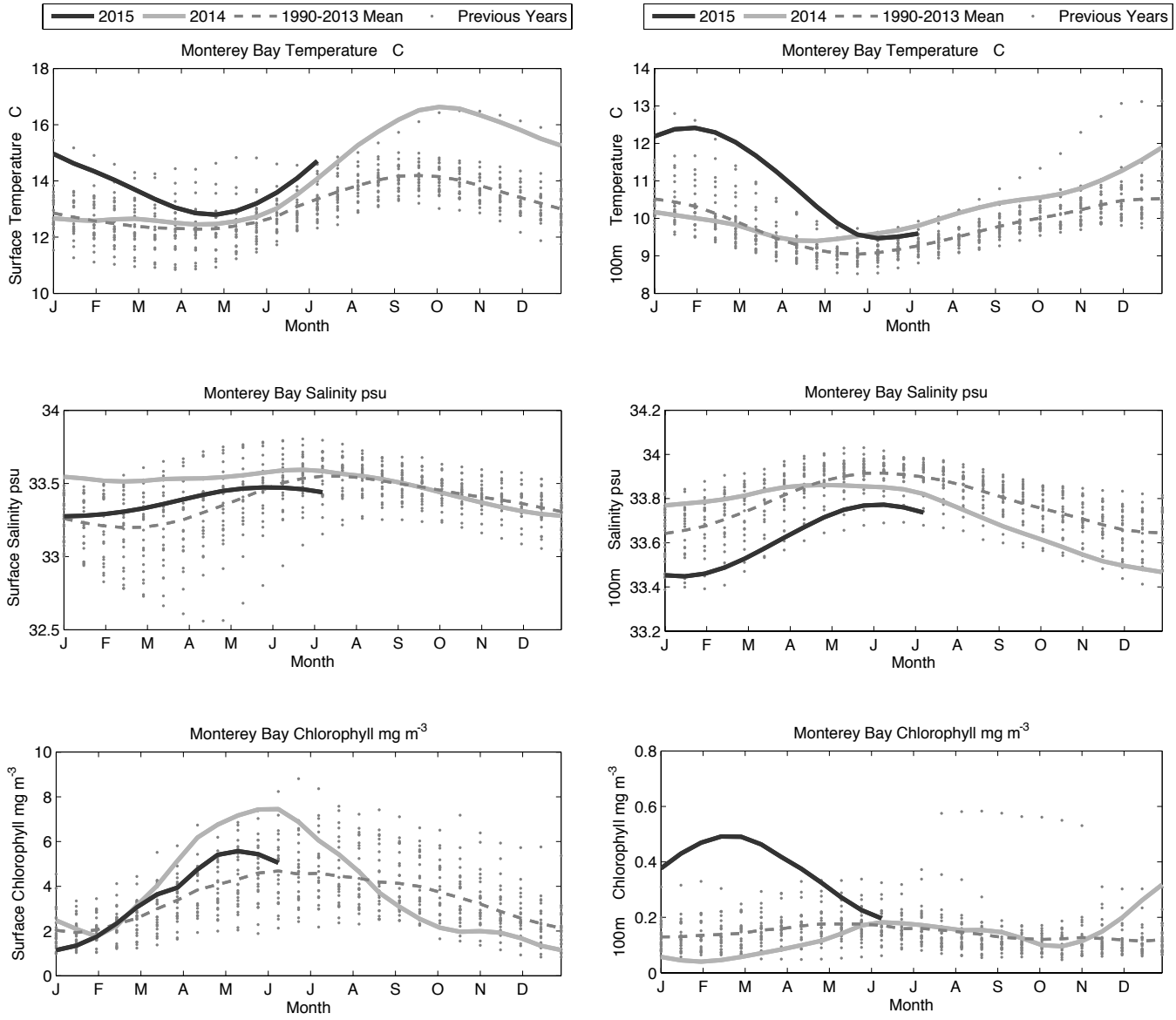

Figure 9. Temperature (top panels), salinity (middle panels) and chlorophyll *a* concentration (bottom panels) at the surface (left-hand column) and at 100 m (right-hand column) observed at the M1 mooring in Monterey Bay, CA.

ing over the shelf in the fall and the decline of the late summer bloom (fig. 8). Coastal waters responded to mild upwelling and storm events during early 2015, and more intense upwelling during spring and summer 2015, yet surface waters often remained relatively strongly stratified throughout the spring and summer. In spring 2015, there was a much stronger phytoplankton bloom (>17 µg chlorophyll *a* L^{-1}). Phytoplankton and water samples collected during spring 2015 confirmed a strong domoic acid event off northern California, and *Pseudo-nitzschia* sp. has remained common into summer 2015.

The copepod community observed off northern California experienced strong shifts in community composition related to changes in hydrographic conditions. Early in 2014, the biomass of copepods with northern biogeographical affinities was similar to past observations, but began to decline in July and dropped dramatically in fall 2014 (fig. 8). Biomass of southern copepods increased during the late summer and fall and remained consistently high through the end of 2014. This pattern of depressed biomass of northern copepods and elevated biomass of southern copepods has persisted through spring 2015. The decline of northern taxa is especially apparent when northern neritic species (including the normally abundant *Pseudocalanus mimus*) are considered separately (data not shown), with strong negative biomass anomalies for the nearshore neritic assemblage persisting through spring 2015. Copepod species richness has

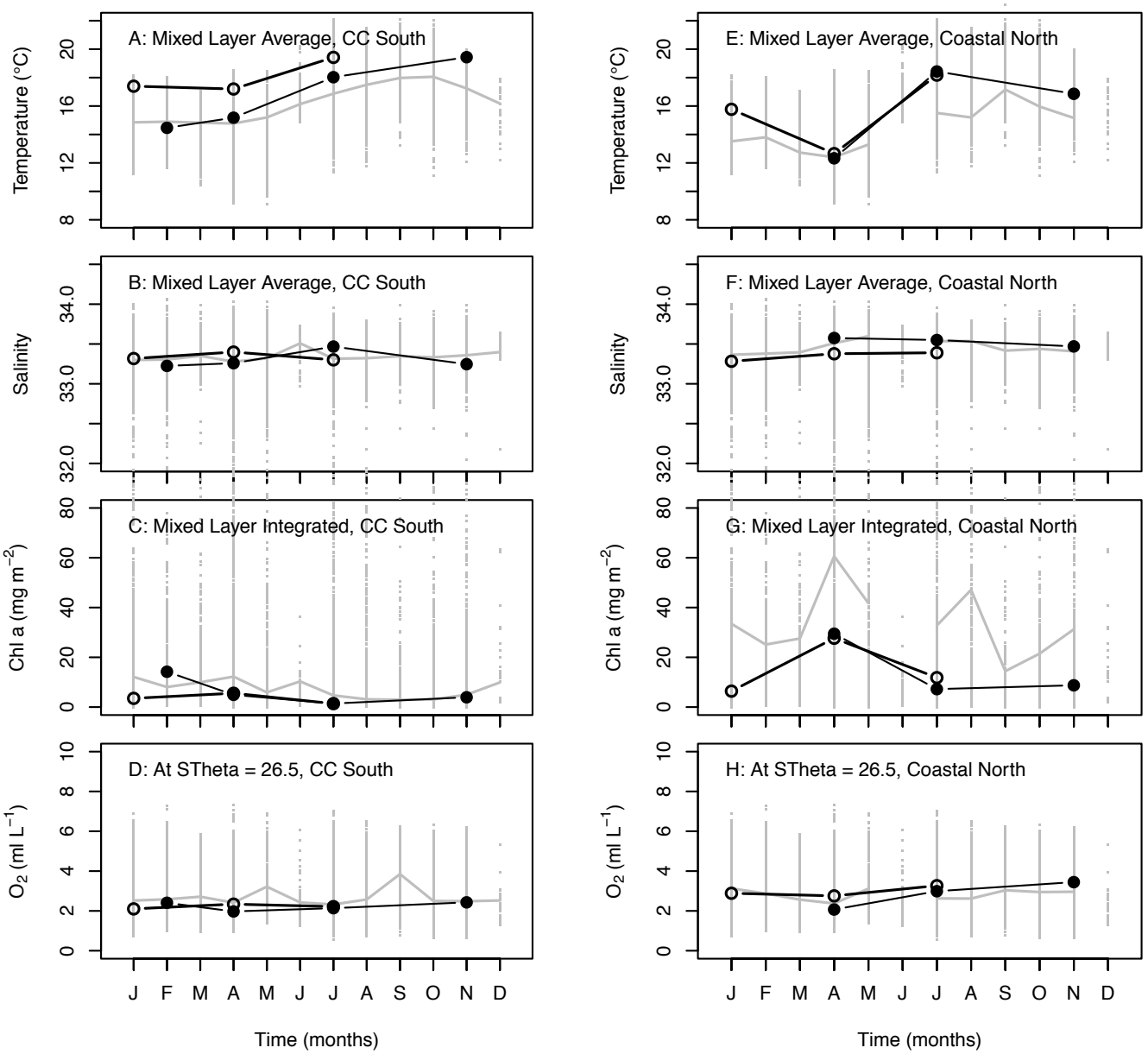

Figure 10. Average mixed layer temperature (A and E), average mixed layer salinity (B and F), integrated mixed layer chlorophyll *a* (C and G), and average O_2 concentration at the σ_θ 26.5 kg m^{-3} isopycnal, from the southern coastal region of the CalCOFI grid (CC south, left-hand column) and the north coastal region of the CalCOFI grid (coastal north, right-hand column). Grey dots show averages for individual cruises from 1984–2013, grey line shows climatological monthly average (1984–2013), line with open symbols shows 2015, and line with closed symbols is 2014. Note, the Feb 2014 cruise was cancelled partway through the cruise due to engine failure, thus there were no samples from the coastal north region.

been consistently high relative to previous years during summer and fall 2014, and again in early 2015 (fig. 8). During this period, several species of southern or offshore copepods have been observed for the first time in the Trinidad Head Line record. Similar patterns are observed in the euphausiid community along the Trinidad Head Line, with substantial declines in *Thysanoessa spinifera*, greater prevalence of offshore species, and the observation of several life history stages of *Euphausia recurva*, a euphausiid that typically occurs well to the south or offshore.

MBARI, M1 Mooring, Central California

Temperatures in Monterey Bay at the surface were some of the highest recorded during fall 2014 since 1990, whereas surface salinities remained near the climatological average during this time period (fig. 9). This contrasts with the rapid warming and freshening seen off Oregon due to the advective intrusion of the blob at that location. Chlorophyll *a* was high at the surface during spring 2014, but declined during the fall. 2015 saw a shift to a fairly different state than previously seen. Chlorophyll *a* values were as high as ever recorded in the

subsurface during the spring, as were subsurface temperatures. However, salinity was also anomalously low, and temperatures anomalously high in the subsurface, suggesting at these depths, there was an intrusion of a different water mass. Surface properties during 2015 were similar to the climatological average.

CalCOFI Surveys, Southern California

The updates to this report are based on four cruises in July and November of 2014 and January and April of 2015. These cruises are part of the CalCOFI program (Ohman and Venrick 2003). Each cruise covers 66 stations off southern California (fig. 1) i.e., the CalCOFI domain, a region that encompasses the southern California Current (sCCS), the Southern California Bight (SCB) and, partially, the coastal upwelling region at and north of Pt. Conception and the edge of the North Pacific Gyre (CalCOFI Lines 90 & 93, Stations 100 to 120). At each station a CTD cast and various net tows are carried out. This report focuses on the hydrographic, chemical, and simple biological data derived from ~20 depths, between the surface and ~515 m, bottom depth permitting. Data from net tows are not available at the present time. For a by-month comparison among years (fig. 10), we divide up the CalCOFI domain following Wells et al. (2013). The first subregion "CC south" denotes the area landward of the main core of the California Current, south of Pt. Conception; essentially the Southern California Bight (CalCOFI lines 87–93, and stations 60–90). The second region "coastal north" denotes the nearshore, upwelling-dominated region from Pt. Conception north to Pt. San Luis (lines 77–80, and stations <60). The third region "edge of North Pacific Gyre" is to the south and offshore, influenced by the subtropical gyre (defined by lines 90–93, and stations 100–120). Within each of these regions, we compared cruise-averaged mixed-layer temperature, salinity, integrated chlorophyll *a*, and oxygen at the σ_θ 26.5 kg m^{-3} isopycnal versus their respective climatological monthly means (based on 1984–2013).

In 2014, within CC south, average mixed-layer (ML) temperatures and salinity were similar to the climatological monthly means (figs. 10A and B, S6), although ML temperatures increased in the fall cruise to >2°C above the mean. ML temperatures were also higher (~ 2°C) in the fall in 2014 in the coastal north region (fig. 10E). Integrated chlorophyll *a* in the CC south was similar to the mean during all cruises, except the early springtime (figs. 10C, S9). In contrast, chlorophyll *a* was anomalously low in the coastal north region during all of 2014, with values typically half their climatological value (fig. 10G). Oxygen at the σ_θ 26.5 kg m^{-3} isopycnal was also similar to the mean in both regions for all of 2014 and 2015 (fig. 10D).

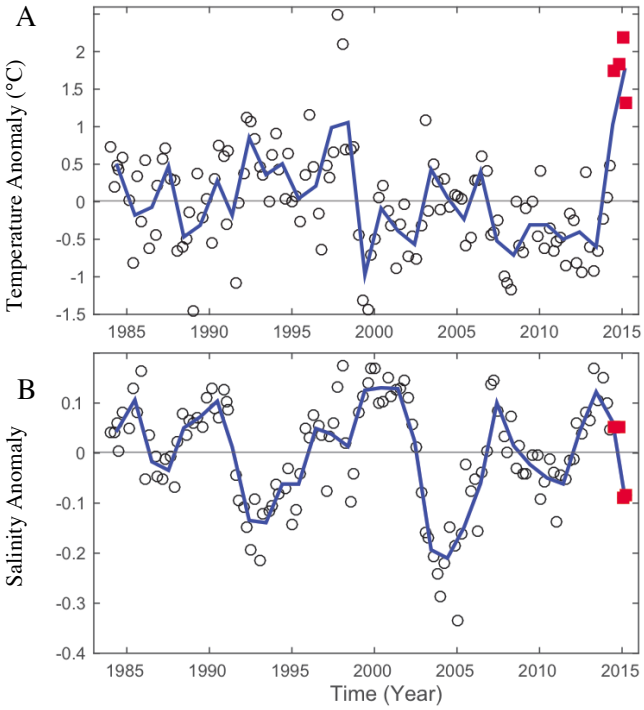

Figure 11. Cruise averages of property anomalies for the mixed layer (ML) of the CalCOFI 66 station standard grid for 1984 to 2015. A: ML temperature; B: ML salinity. Data from individual CalCOFI cruises are plotted as open circles; data from the four most recent cruises, 201407 to 201504, are plotted as solid red squares. Thin solid blue lines represent annual averages, grey horizontal lines the climatological mean, which is zero in the case of anomalies. Anomalies are based on the 1984 to 2012 time period.

In 2015, within the CC south region, ML temperatures were on average >3°C warmer than the climatological mean from winter through spring (fig. 10A). ML temperatures in the north coastal region were warmer than average in the winter, and summer, but not the spring cruise, as there was some limited upwelling in that region during that time (figs. 10E and 2). Chlorophyll *a* was again approximately half that of the climatological mean for both the south and north coastal regions during the 2015 cruises (figs. 10C and G).

For time series analysis (figs. 11 and 12), observations were averaged over all 66 stations covered during a cruise. Anomalies (fig. 11) were calculated comparing these averages with respect to the 1984–2012 time period. The mixed-layer depth is calculated using a density criterion and is set either to 10 m or to the half-way point between the two sampling depths where the sigma-theta gradient first reaches values larger than 0.001 kg m^{-3} per meter, whichever is larger. The nitracline depth is defined as the depth where concentrations of nitrate reach values of 1 μM, calculated from measurements at discrete depths using linear interpolation. Methods used to collect samples and analyses carried out on these samples are described in detail at calcofi.org/methods. Regressions of time series were

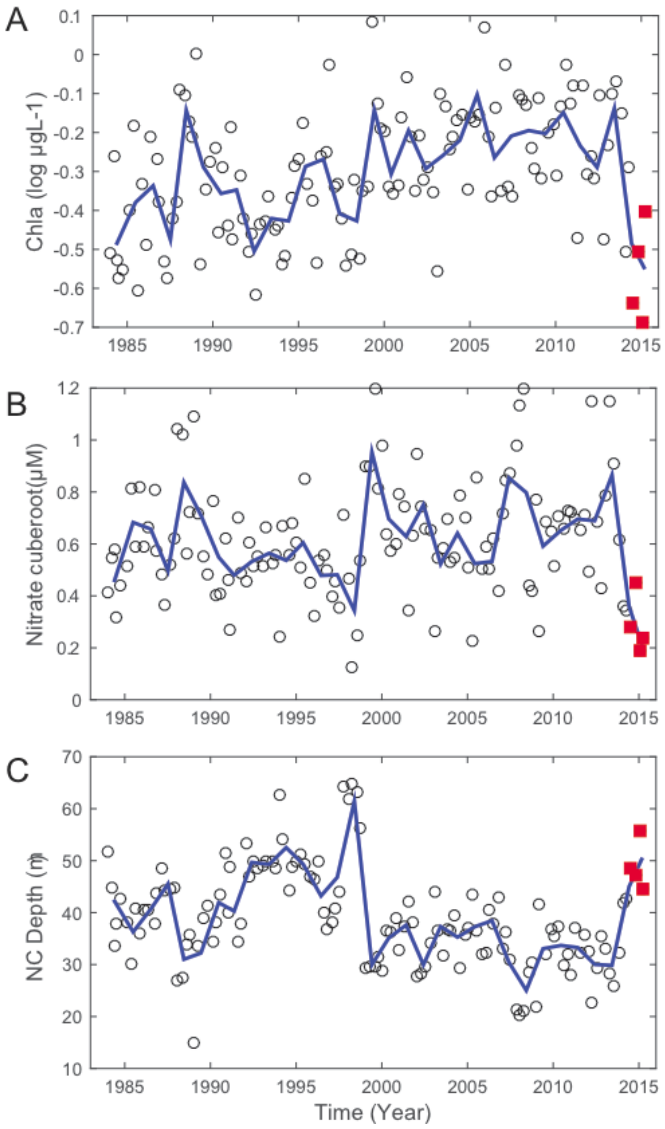

Figure 12. Cruise averages of properties for a depth of 10 m for the CalCOFI standard grid. A: The log10 of chlorophyll *a*, B: the cube root of nitrate, and C: nitracline depth. Data are derived and plotted as described for Fig. 11.

carried out in MATLAB's System Identification toolbox, which follows Ljung (1999).

Over the last 12 months ML temperatures off southern California were as high as those observed during the 1998 El Niño (fig. 11A), a clear expression of the Southern California Warm Anomaly (SCWA; geographically distinct from the NE Pacific blob). Significant near-surface (10 m) warm relative anomalies (which are standardized anomalies and therefore dimensionless) were first observed during the spring of 2014 along the continental shelf break (figs. 36A and B), on the order of 1.5 standard deviations larger than the long-term mean. The winter 2014 cruise did not cover the whole CalCOFI grid, only Lines 93 and 90. Relative temperature anomalies along Line 90 (see below) had values of 0.8 units during this cruise, compared to values of 1.7 during the spring cruise. The relative anomalies intensified in the summer of 2014 in the SCB and were particularly strong SW off Pt. Conception (fig. 36C), reaching values of 4 units. It is unlikely that these high anomalies are entirely due to the in situ warming of the surface layer. Upwelling during July and August of 2014 was unusually low at 33°N (fig. 2); thus the "absence" of cold water, often present off Pt. Conception due to upwelling (e.g., fig. 36C), contributed to the extremely large anomalies during the summer of 2014. By the fall of 2014 large positive anomalies were observed throughout the study domain and these reached highest values during the winter of 2015 (fig. 36E), when the average relative temperature anomaly was 2.2 with values at individual stations ranging from 1.2 to 3.7 units. During the spring of 2015 relative anomalies were still very strong in the California Current proper and in the southern part of the study domain. The decrease in ML salinity (fig. 11B) over the last 12 months is primarily due to decreased salinity in the California Current region; relative changes of ML salinity in coastal and offshore areas were not as large (fig. S7). Similar patterns, i.e., salinity changes primarily driven by the waters of the CCS, were observed during the 2012 salinity minimum (Wells et al. 2013). Spatial distributions of these properties for the individual cruises can be found at calcofi.org/publications.

Plots of ML chlorophyll *a* and ML nitrate (NO_3) vs. time are difficult to interpret because distributions of the data are skewed. This can be avoided using a log-transform for the chlorophyll *a* data and a cube-root transform for the NO_3 data (the latter to effectively deal with zero values of nitrate). Such transformations will place heavy emphasis on the variability of these parameters when their values are low. Values of ML log chlorophyll *a* during the SCWA were the lowest observed during the 1984 to 2015 time period (fig. 12A). Cruise averages of cube-root NO_3 during the SCWA were almost as low (fig. 12B). Annual ML chlorophyll *a* and nitrate averages show great coherence over time, and significant correlations (Autoregressive Exogenous, ARX [1 2 0] model) at lags of zero ($p < 0.01$) and one ($p < 0.01$) year. This correlation suggests that, during the SCWA, phytoplankton biomass was controlled by the availability of NO_3 or a nutrient co-varying with NO_3. Similar conclusions have been reached for low phytoplankton biomass during strong El Niño events in the southern California Current system (Hayward 2000). Low ML concentrations of NO_3 are likely controlled by stratification, as a comparison of cube-root NO_3 and nitracline depth (NC depth, fig. 12B, C) shows.

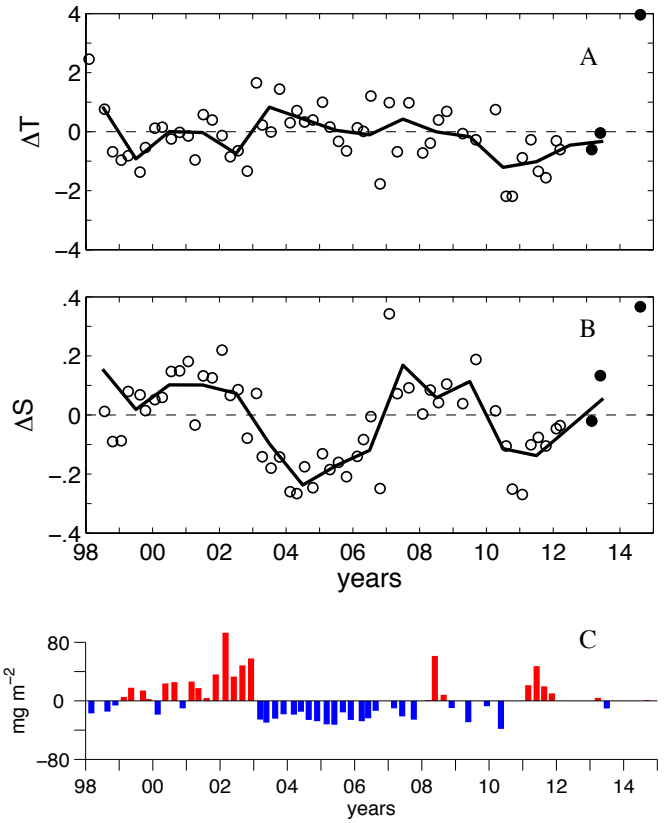

Figure 13. A) Mixed layer temperature (°C), and B) salinity (g kg^{-1}) anomalies off the Baja California Peninsula (IMECOCAL grid). Each symbol represents the average anomaly for each cruise conducted. Data from the 2013 and 2014 surveys are plotted as solid symbols. The thick solid line indicates annual average. C) Time series of 0–100 m integrated chlorophyll-*a* anomalies for the IMECOCAL region. Each bar represents the anomaly of a single cruise.

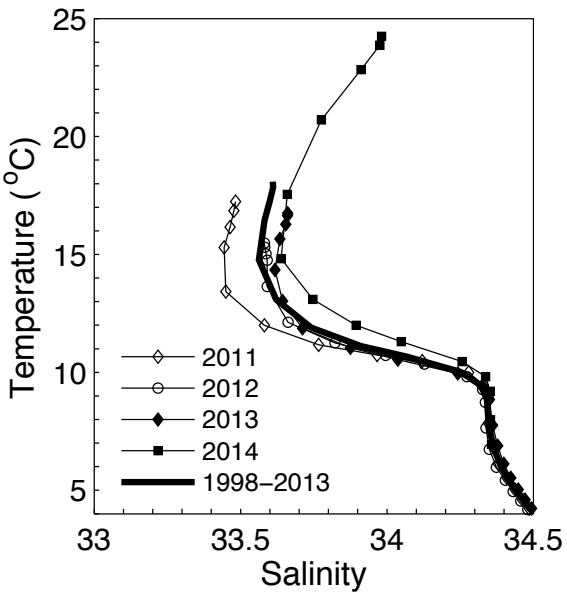

Figure 14. Annual mean T-S curves for the period 2011–13 of the IMECOCAL region. The curve labeled 2014 refers to the cruise mean values of summer 2014. The long-term mean (1998–2013), is indicated by the thick line. Each data point indicates one standard depth, from the surface to 1000 m.

IMECOCAL Surveys, Baja California

During 2014, a single summer cruise occupying a total of 85 hydrographic stations was conducted off the Baja California Peninsula by the IMECOCAL program (fig. 1). Contrasting to near normal mixed-layer temperatures in the previous year, summer 2014 depicted the presence of water up to 4°C warmer relative to the long-term mean (fig. 13A). Following the same regional trend, mixed-layer salinities also showed larger than normal values, with anomalies of ~0.4 g kg^{-1} (fig. 13B). As suggested by the temperature-salinity diagram (fig. 14), the influence of warmer and saltier waters during summer 2014 was apparently restricted to the upper 50 m. Below this depth, the TS curve follows closely the 1998–2013 climatological mean and the near-normal conditions observed during 2012 and 2013. The warming of the mixed-layer depicted in figures 13 and 14 was most conspicuous for latitudes south of Punta Eugenia, where near-surface warmer waters were evident since early 2014, and where the largest temperature and salinity anomalies (>5°C and ~0.7 g kg^{-1}, respectively) were observed near shore (data not shown). Dynamic height anomaly calculations indicated poleward alongshore flows in the southern region, typical for the summer season (Durazo 2015). As is commonly observed during warm events (Durazo and Baumgartner 2002), these flows were not evident north of Punta Eugenia. Water-column integrated phytoplankton chlorophyll *a* (0–100 m) continued with near normal conditions observed in previous years, with negligible anomalies in 2014 (fig. 13C).

REGIONAL PATTERNS IN FISH SPECIES

Northern California Current, Newport Line

Ichthyoplankton samples were collected from 3–4 stations representing coastal (<100 m in depth), shelf (100–1000 m), and offshore (>1000 m) regions along both the Newport Hydrographic (NH; 44.65°N, 124.35–125.12°W) and Columbia River (CR; 46.16°N, 124.22–125.18°W) lines off the coast of Oregon between June 15 and July 20 in 2007–14 (for complete sampling methods, see Auth 2011). In addition, post-larval (i.e., juvenile and adult) fish were collected using a modified-Cobb midwater trawl (MWT). MWT collections were made at 4–6 evenly-spaced, cross-shelf stations representing coastal, shelf, and offshore regions along nine half-degree latitudinal transects between 42.0° and 46.0°N latitude in the northern California Current region during June–July in 2011–15 (although no sampling was conducted in 2012).

The ichthyoplankton community in the central-northern coast of Oregon in June–July 2014 was simi-

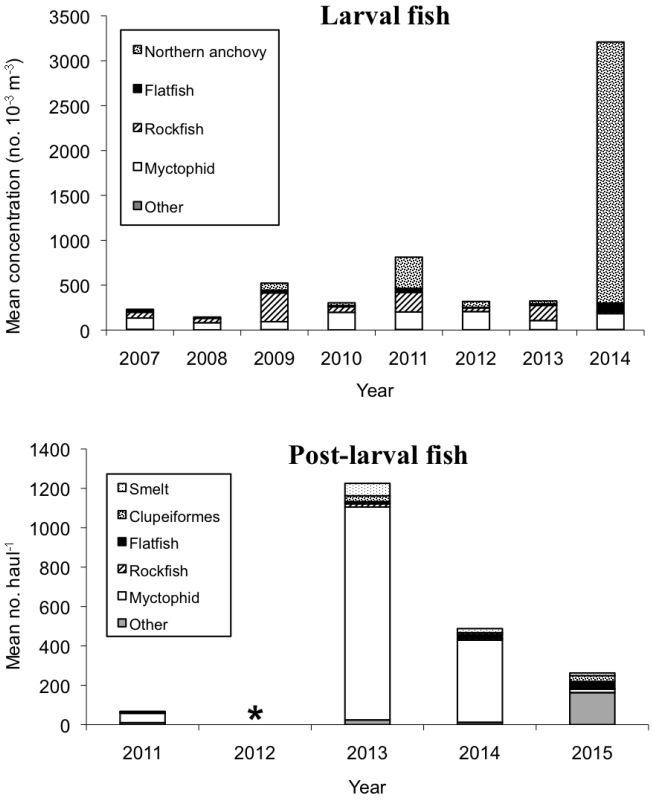

Figure 15. A) Mean concentrations (no. 10^{-3} m^{-3}) of the dominant larval fish taxa collected during June–July in 2007–14 along the Newport Hydrographic (NH; 44.65°N, 124.35–125.12°W) and Columbia River (CR; 46.16°N, 124.22–125.18°W) lines off the coast of Oregon. B) Mean catches (no. $haul^{-1}$) of the dominant post-larval fish taxa collected during June-July in 2011–15 along nine half-degree latitudinal transects between 42.0 and 46.0°N latitude in the northern California Current region. * = no samples were collected in 2012.

lar to the average community structure found in the same area and season during the previous seven years in terms of composition and relative concentrations of the dominant taxa, with the exception of the unusually high concentration of northern anchovy, which dominated the ichthyoplankton at a mean concentration that was >16x higher than that of the next highest taxon, myctophids (fig. 15A). Larval northern anchovy and flatfish in 2014 were found in concentrations >8x and >2x higher, respectively, than those of the next highest year in the time series, 2011, while larval rockfish were found in concentrations >2x lower than the next lowest year in the eight-year time series, 2012.

The post-larval fish community in the northern California Current in June–July 2015 differed from the community structure found in the same area and season in 2011–14 primarily due to the low numbers of myctophids found in 2015, which normally are the dominant taxon in the fish community, and the increased abundance of "other" taxa relative to previous years, which is an indicator of increased diversity in 2015 (fig. 15B). The abundance of flatfish in 2015 was the highest of the four-year time series, while that of rockfish was the lowest. The abundances of smelt and clupeiformes in 2015 were about average for the time series.

Northern California Current, Oregon and Washington Coast

Biomass of available fish prey for out-migrating juvenile salmon in 2015 is predicted to be above average based on the winter ichthyoplankton biomass index (Daly et al. 2013) primarily due to an anomalously high biomass of northern anchovy and rockfish larvae. This winter (January to March) biomass of fish larvae that salmon prey upon was the fourth highest in the last 18 years (fig. 16). The biomass of fish larvae in late winter provides an index of juvenile fish that are the common prey of juvenile salmon when they enter the ocean in spring and summer. Due to the anomalously warm ocean conditions during the winter of 2014–15, which typically predict lower salmon survival of early ocean migrants, we are uncertain about the accuracy of the current prediction for salmon returning in 2016 and 2017. The overall composition of winter ichthyoplankton that are important prey for salmon in 2015 was most closely aligned with 2004 and 2005, both poor outmigration survival years. While the biomass in 2015 predicts returns of spring Chinook salmon to Bonneville Dam at slightly over 200,000 adult fish, the ichthyoplankton composition based on axis ordination scores predicts 93,000 adult fish returning in 2017, which is the largest discrepancy in these two predictors over the 18 years of the survey. Warm winter ocean conditions observed in both 2014, and especially early 2015, indicate poor returns of adult salmon in the next few years. Also noteworthy in the winter ichthyoplankton collections for 2015 were that: 1) three new offshore taxa were collected, 2) there were larvae present at all sampling stations, 3) and there were high concentrations and biomass of Pacific sardine larvae in February and March from NH–01 (most inshore station) to NH–25 (most offshore station), all of which had not occurred prior to 2015 (fig. 15A). While northern anchovy larvae have previously been collected in January–March along the NH line (in March 1998 and 2003), their 2015 biomass was over 100 times greater than in any previous year, and as with the Pacific sardine larvae, northern anchovy larvae were present all across the shelf from inshore to offshore stations (NH–01 to NH–25; Auth et al. in prep).

Catch per unit effort (CPUE, number per km trawled) of most juvenile salmonids during this survey was lower than average compared to the 16 previous June surveys 1998–2013 (fig. 17). Catches of yearling Chinook salmon (*Oncorhynchus tshawytscha*) in June 2014 were ninth of the 17 years of sampling, and catches of yearling coho salmon (*O. kisutch*) were ranked 10 out of

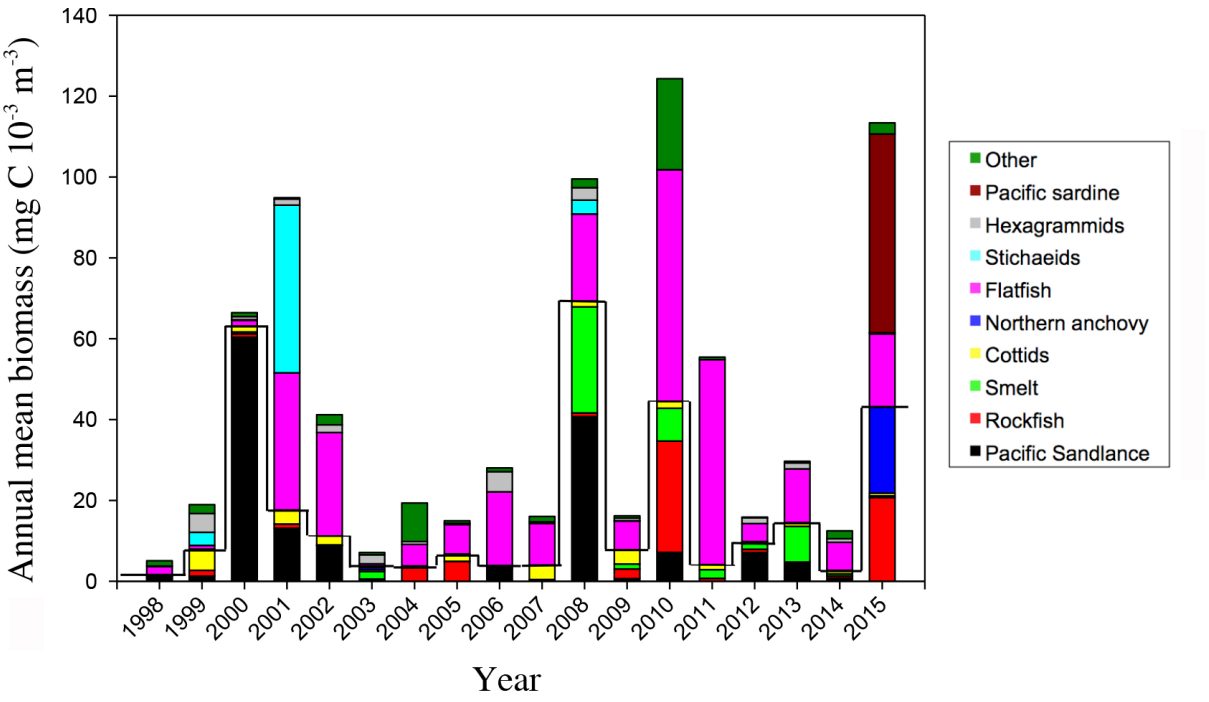

Figure 16. Annual mean biomass (mg C 10^{-3} m^{-3}) of the five important salmon prey taxa (below solid line) and five other dominant larval fish taxa (above solid line) collected during winter (January–March) in 1998–2015 along the Newport Hydrographic (NH) line off the coast of Oregon (44.65°N, 124.18–124.65°W). Figure expanded from one presented in Daly et al. (2013).

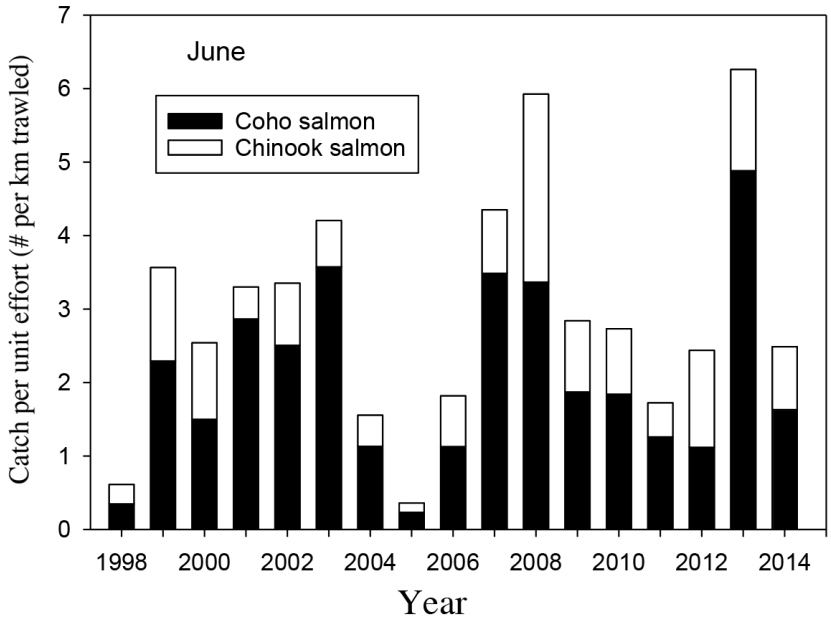

Figure 17. June salmon catch (catch per unit effort, CPUE, number per km trawled). Catches of juvenile coho (black bars) and Chinook (white bars) salmon off the coast of Oregon and Washington in June from 1998–2014.

17 years. The abundance of yearling Chinook salmon during June surveys has a significant and positive relationship to spring Chinook jack counts at Bonneville the following spring. The abundance of yearling coho salmon during these surveys also has a significant and positive relationship to coho smolt to adult survival. Thus, catches of yearling salmon in June may be a good indicator of first year ocean survival of yearling Chinook and coho salmon.

Pelagic fish and invertebrate catch data were collected by the NWFSC-NOAA Bonneville Power Administration survey surface trawls on standard stations along transects between La Push, WA, and Newport, OR, in June from 1999 to 2015. All tows were

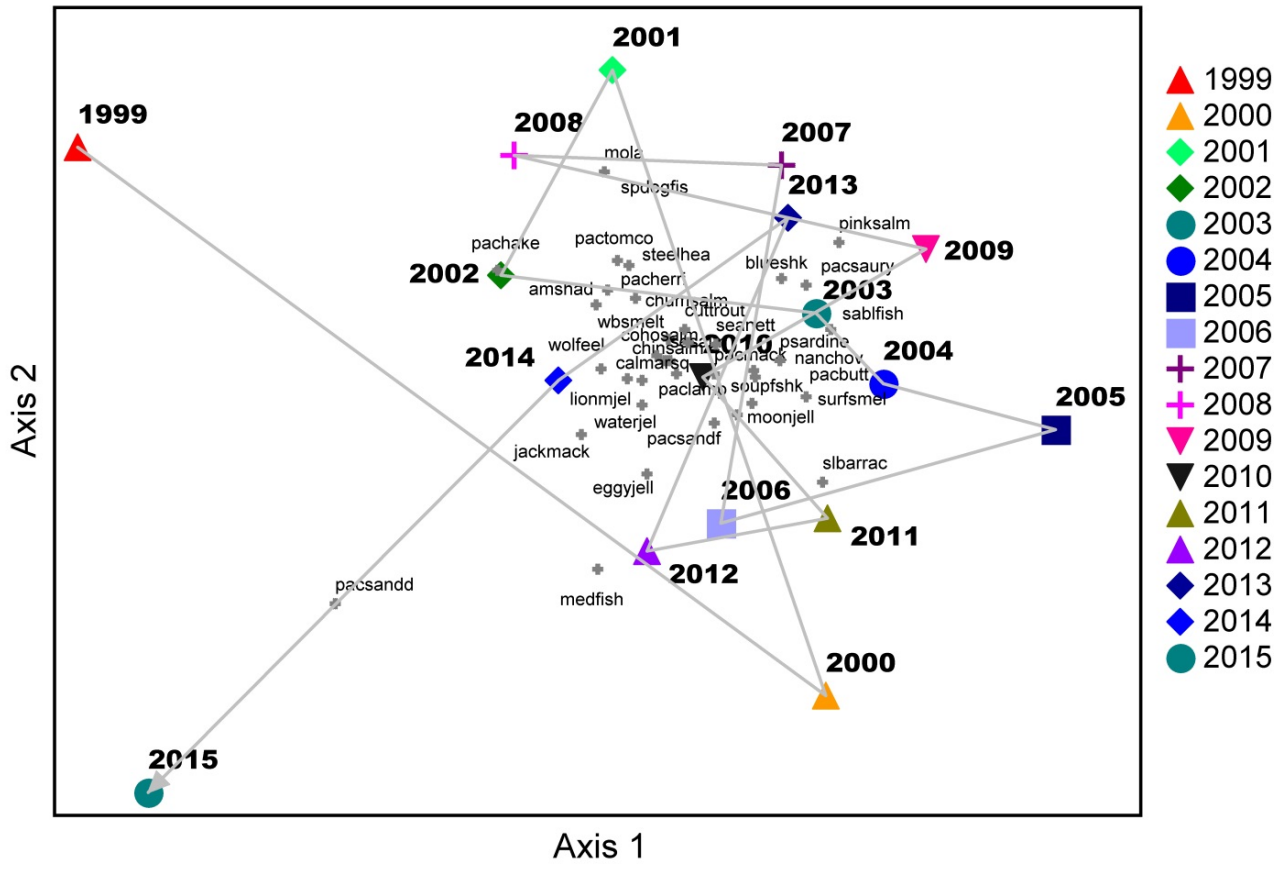

Figure 18. Nonmetric multidimensional scaling plot of the 36 most commonly-occurring taxa from the NWFSC-NOAA June pelagic fish surveys from the Northern California Current. Shown are the individual years as symbols, which are connected by a progressive vector and an overlay of the taxa that contribute to the variation seen in the plot. Final stress of the ordination was 13.898.

made during the day at predetermined locations along transects extending off the coast to the shelf break (Brodeur et al. 2005). We restricted the data set to stations that were sampled more than 9 years over the sampling time period. Numbers of individuals were recorded for each species caught in each haul and were standardized by the horizontal distance sampled by the towed net as CPUE (#/km^2 towed; units are calculated as the width of the trawl opening, 0.03 km, multiplied by the distance towed, in km. Height of the trawl gear was not measured during every cruise, and was thus not used in these calculations, but is estimated at 0.02 km). Yearly abundance data were obtained by averaging the standardized CPUE data across stations for each species sampled during the June surveys. We restricted the species data to the 36 most abundant species captured in this data set over the 17 years sampled. We applied a log(x+1) transformation to the species x year data set (36 species x 17 years), on which we ran a nonmetric multidimensional scaling (NMS; Kruskal 1964) ordination to describe the similarity of each year's community in species space.

The resulting NMS ordination explained 87.4% of the total variability in the first two dimensions, with NMS axes 1 and 2 explaining 64.1% and 23.3% of the variability, respectively. Although the community for 2014 had lower axis 1 scores than most of the previous years of sampling, it was not extreme, particularly compared to 2015 (fig. 18). The community of fish and invertebrates in June 2015 had the lowest value for axis 2 and the second lowest (slightly less than 1999) for axis 1. Although the main taxa most indicative of the relationship was Pacific sanddabs (*Citharichthys sordidus*), other taxa were more abundant than normally found in previous June cruises including jack mackerel (*Trachurus symmetricus*), California market squid (*Doryteuthis opalescens*), and several jellyfish taxa (water jellyfish, *Aequorea* sp.; egg yolk jellyfish, *Phacellophora camtschatica*). Several of the forage fish species typically found in these surveys, such as Pacific herring (*Clupea pallasi*), northern anchovy (*Engraulis mordax*), and smelts (family Osmeridae) and most salmonids were found in much lower abundances in 2015 than previous years. Large gelatinous zooplankton taxa have been quantified in large pelagic surface trawls off Oregon and Washington every June since 1999 (see Suchman et al. 2012 for collection methods). The normally dominant Scyphozoan species, *Chrysaora fuscescens*, has shown a decrease in abundance since the El

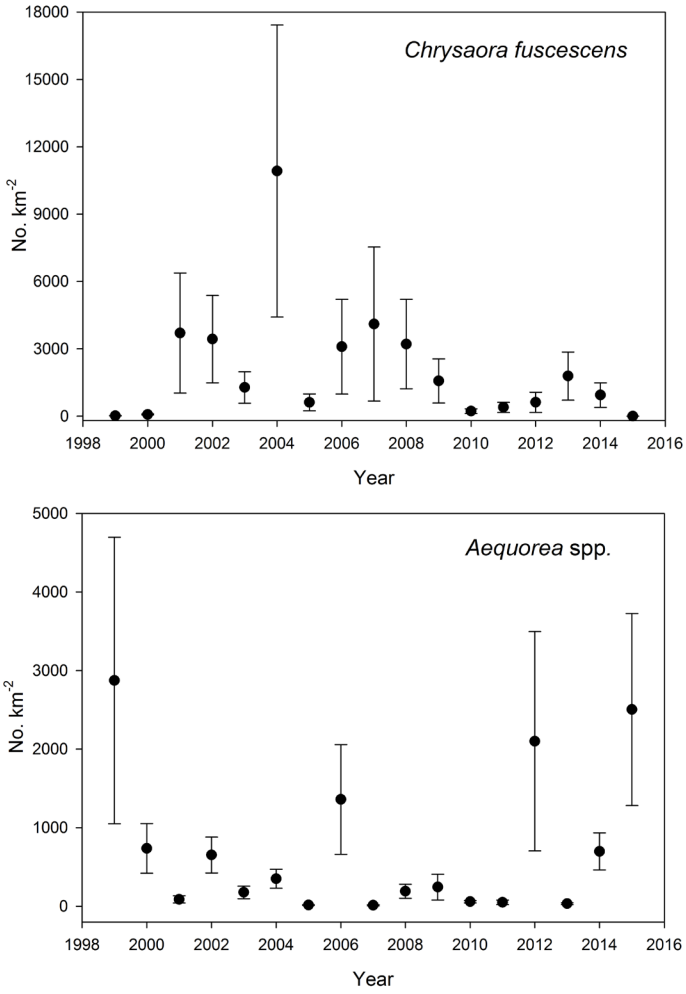

Figure 19. Catches of the dominant jellyfish taxa in pelagic surveys off the coast of Washington and Oregon in June from 1999 to 2015. Data are the means and standard deviations of the catch per km² of (a) *Chrysaora fuscescens* and (b) *Aequorea* spp. in the entire survey area.

Niño of 2010 and, in fact, was found in the lowest abundance of the time series in June 2015 (fig. 19), occurring in less than 25% of the stations sampled, mostly at the nearshore stations (<15 km from shore). The smaller Hydromedusae, *Aequorea* sp., is generally found in much lower densities at the offshore stations (Suchman et al. 2012) but was by far the numerically dominant taxa in 2015. Other offshore and/or southern species such as the large scyphozoan, *Phacellophora camchatica*, the pleustonic *Velella velella*, and colonial salps (*Salpa* and *Thetys*) were found during the warm ocean conditions that occurred in 2015 leading to a gelatinous faunal composition that resembled that of an El Niño year.

Ecosystem indicators for the Central California Coast, May–June 2014

The Fisheries Ecology Division of the SWFSC has conducted an annual midwater trawl survey for pelagic juvenile (young-of-the-year, YOY) rockfish (*Sebastes* spp.) and other groundfish off of central California (approximately 36° to 38°N) since 1983, and has enumerated most other pelagic micronekton encountered in this survey since 1990 (Ralston et al. 2013; Ralston et al. 2015). The survey, conducted in late spring (May–June), expanded the spatial coverage to include waters from the US/Mexico border north to Cape Mendocino in 2004. The primary objectives are to estimate the abundance of YOY rockfish and other groundfish for stock assessments and fisheries oceanography studies, but the survey also quantifies trends in the abundance and composition of other components of the micronekton forage assemblage (including other juvenile fishes, krill, coastal pelagic species, and mesopelagic species), as well as the collection of oceanographic information (CTD casts, continuous data on surface conditions and productivity, and acoustic data) and seabird and marine mammal abundance data. The results here include time series of anomalies of some of the key species or groups of interest in this region since 1990 (core area; fig. 1, right-hand panel, letter A) or 2004 (expanded survey area), and an update of a principal component analysis (PCA) of the pelagic micronekton community in the core area developed by Ralston et al. (2015), all of which have also been reported in earlier SoCC reports. The data for the 2015 survey are preliminary, and corrections have been made in catch data for previous years, which have resulted in very slight changes to overall abundance trends.

The standardized anomalies from the mean of the log (x+1) catch rates are shown by year for six key YOY groundfish and forage groups (fig. 20), including all YOY rockfish, market squid (*Doryteuthis opalescens*), krill (primarily *Euphausia pacifica* and *Thysanoessa spinifera*), YOY Pacific sanddab (*Citharichthys sordidus*), Pacific sardine (*Sardinops sagax*) and northern anchovy (*Engraulis mordax*). The 2015 data generally show a continuation of the very high catches of juvenile rockfish and Pacific sanddab (fig. 20; top left and middle right) in the core, southern and northern California areas (fig. 1, right-hand panel, letters A, B, and C, respectively); in fact in both the core and southern areas mean catches were the highest observed in the entirety of the time series. However, the abundance of krill (fig. 20; middle left) was at or below average levels for all regions, and the abundance of adult Pacific sardine and northern anchovy (fig. 20; bottom panels) remained very low as well (although larval catches for both species were at high or record levels in most areas). The abundance of market squid continued to remain very high in the core area, although catches were lower in the southern region where the bulk of the market squid fishery takes place (fig. 20; top right). Catches of octopus, lingcod (*Ophiodon elongates*), Pacific hake (*Merluccius productus*), and several other groundfish were also high. North of Cape Mendocino, catches of

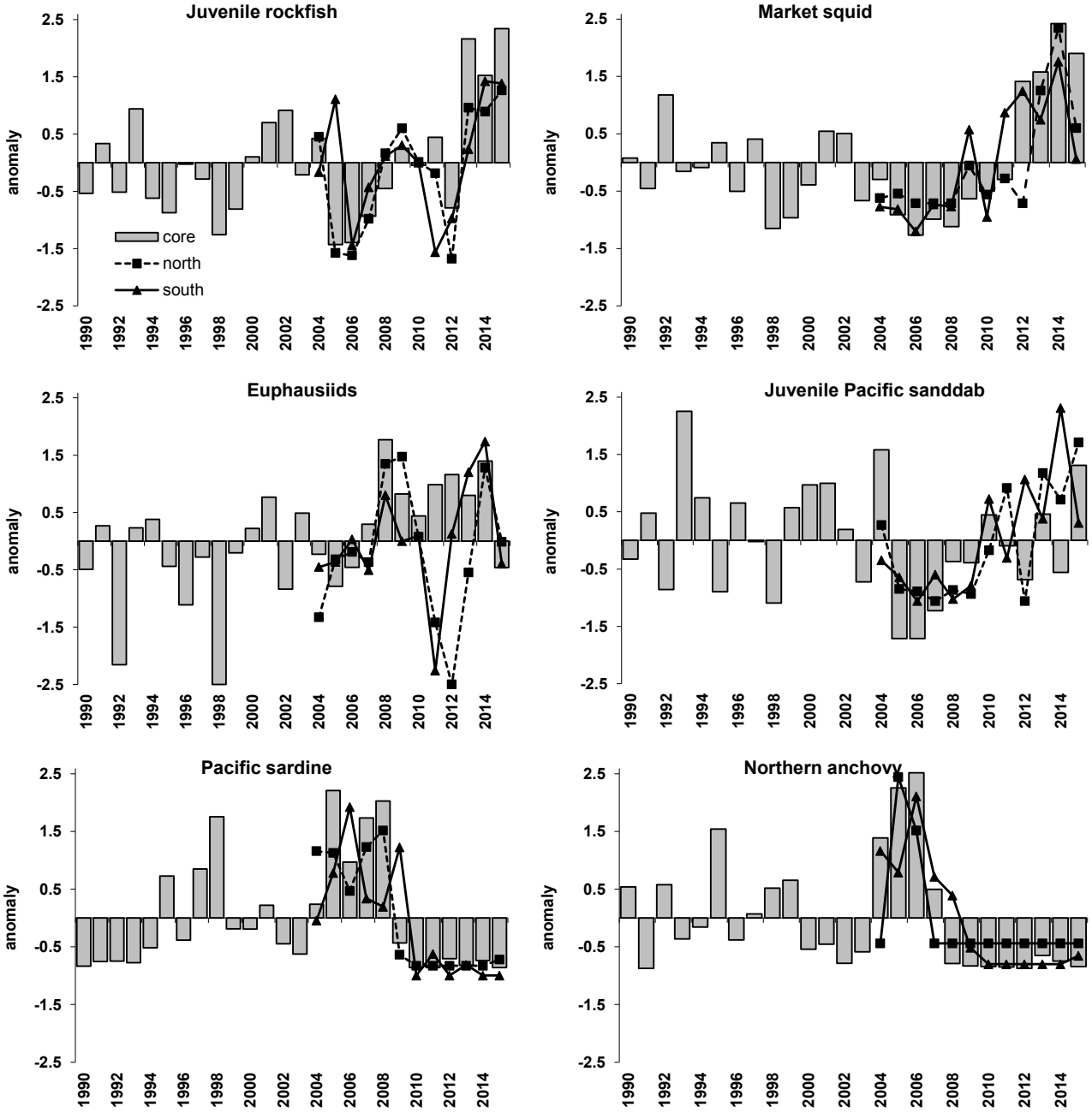

Figure 20. Long-term standardized anomalies of several of the most frequently encountered pelagic forage species from rockfish recruitment survey in the core (central California) region (1990–2015) and the southern and northern California survey areas (2004–15, excluding 2012 for the northern area).

YOY rockfish and other groundfish were at very low levels in both 2014 and 2015 (R. Brodeur, unpublished data), consistent with occasionally dramatic differences in catch rates of YOY rockfish over broader spatial scales (Ralston and Stewart 2013).

In addition to the high catches of YOY rockfish and other groundfish, catches tended to be very high for a suite of both less commonly encountered and less consistently reported (over the course of the time series) species. Although catches of scyphozoan jellyfish (primarily *Aurelia* spp. and *Chrysaora* spp.) were unusually low in 2015 (fig. 21), catches of pelagic tunicates (primarily *Salpa* spp., *Thetys vagina* and *Pyrosoma* spp.) were at extreme to record high levels. Finally, despite the high abundance (inferring high productivity and transport of subarctic water) of both YOY groundfish and of pelagic tunicates, the 2015 survey also encountered unusually high numbers of warm water species (many of which had never previously been encountered), which are typically considered to be harbingers of strong El Niño

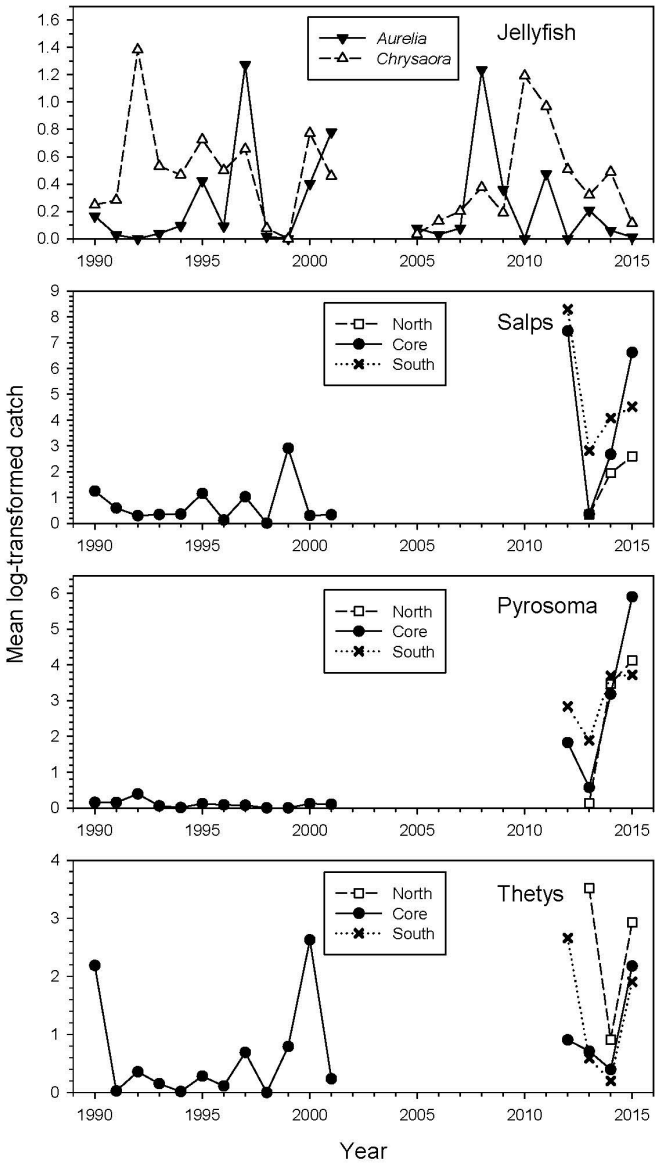

Figure 21. Standardized catches of jellyfish (*Aurelia* spp. and *Chrysaora* spp.) in the core area and pelagic tunicates in the expanded survey area.

events, northward transport of subtropical waters, and unusually low productivity. These included record-high numbers of pelagic red crabs (*Pleuroncodes planipes*), California spiny lobster (*Panulirus interruptus*) phyllosoma (pelagic larvae), and the largely subtropical krill *Nyctiphanes simplex*. Additionally, these included the first time catches (in this survey) of the greater argonaut (*Argonauta arga*), the slender snipefish (*Macroramphosus gracilis*), and the subtropical krill *Euphausia eximia*. The 2015 survey was highly unusual in that species characteristic of all three of what might very generally be considered nominal states (YOY groundfish dominated catches, pelagic tunicate dominated catches, and subtropical species dominated catches) were encountered in high abundance throughout this region.

In addition to the six species shown in fig. 20, an additional 14 species and groups were included in the analysis of the forage assemblage within the core (1990–2015) area (fig. 1; right panel, letter A) developed by Ralston et al. (2015), and are subsequently represented in the PCA of this assemblage. The additional YOY groundfish groups include Pacific hake, speckled sanddab (*C. stigmaeus*), rex sole (*Glyptocephalus zachirus*), and lingcod. The remaining species and groups in the assemblage include adult Pacific hake, octopus, sergestid shrimp, gobies, plainfin midshipman (*Porichthys notatus*), and a variety of mesopelagic species. Of those that are included, YOY groundfish, market squid, krill and several other taxa had strong positive loadings on PC1 (which explained 32% of the total variance, the first three PCs explained a total of 60% of the variance), with northern anchovy, Pacific sardine and most mesopelagic species loading negatively. This PC was not significantly related to basin-scale environmental indicators such as the PDO, MEI, and the NPGO, but rather was strongly related to both localized physical conditions (temperature, salinity, density and depth of the 26.0 sigma theta isopycnal; see also Santora et al. 2014) and indicators of large-scale transport (AVISO sea surface height anomalies), such that the YOY rockfish, market squid, and krill groups were more abundant during cool, high transport conditions. The second PC tended to load more strongly on the mesopelagic community, but related poorly to environmental indicators, while PC3 had strong loadings on a suite of taxa and was highly correlated to basin-scale climate indicators (see Ralston et al. 2015 for details). Unfortunately, the pelagic tunicates have not been consistently quantified over the time period of the survey, while the subtropical species are typically rare and therefore did not meet the minimum percentage of frequency of occurrence (10%) from the analysis. Thus, those groups are not represented in the PCA results.

The two leading PCs for the assemblage are shown in a phase plot as Figure 22, and the dramatic (and apparently ongoing) separation of the 2013 through 2015 period is noted as being on the opposite end of the PC1 scale compared to the low productivity years of 1998, 2005, and 2006. Such shifts have important implications for higher trophic level species, such as seabirds, marine mammals, salmon, and adult groundfish that forage primarily or exclusively on one or another component of this assemblage. The observed dynamics of the YOY groundfish and high turnover invertebrates is thought to largely represent shifts in productivity associated with higher survival (recruitment) of early life history stages for these species, while the trends observed for coastal pelagic and mesopelagic species (which load negatively on PC1 and positively on PC2) are thought to be related to both variability in abundance as well as shifts in their

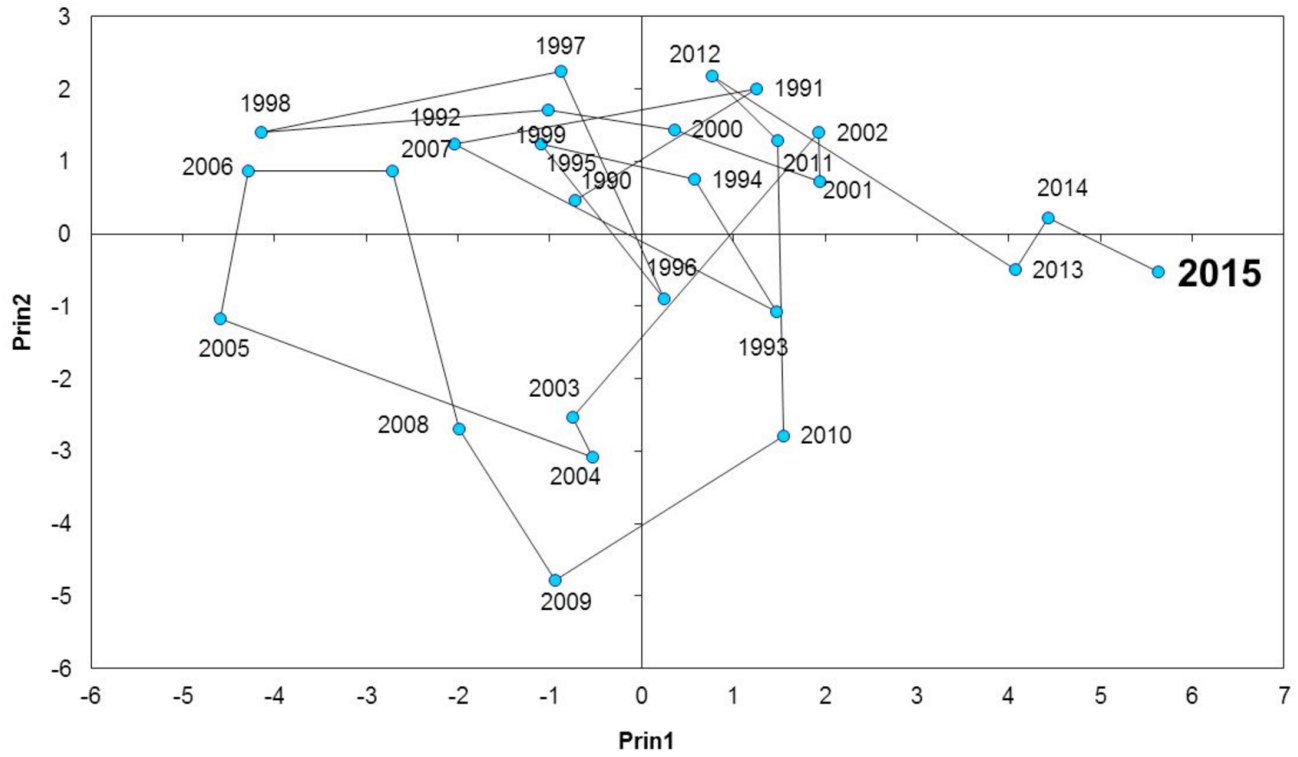

Figure 22. Principal component scores plotted in a phase graph for the twenty most frequently encountered species groups sampled in the central California core area in the 1990–2014 period.

distribution and consequent availability to the midwater trawl. Yet overall the results of the PCA clearly indicate that in the core area, and presumably in the northern and southern regions as well, the micronekton community composition is highly unusual relative to those observed throughout the history of this survey.

Ecosystem Indicators for the Southern California, CalCOFI Region

Coastal pelagic fish egg abundance has declined off central and southern California in the last 15 years (2000–15) (fig. 23). Sardine, anchovy, and jack mackerel eggs were found at very low concentrations in the spring of 2015. Although peak anchovy spawning occurs in December–February, which is earlier than the March–April spring survey, the anchovy spawning that extends into spring shows the same trend to lower egg densities as do sardine and jack mackerel. Anchovy and jack mackerel are lightly fished, and although commercial catches of sardine are higher, the observed decline in egg densities of all three species suggests that environmental factors are likely to be the major cause of the decline in spawning of these forage fishes.

Jack mackerel eggs were an order of magnitude more abundant than sardine or anchovy eggs in spring 2015 (fig. 24). Despite their relatively higher abundance, jack mackerel eggs were less abundant than during every spring in the last 15 years, except for 2010–12 (fig. 23). The distribution of jack mackerel eggs in 2015 was also more restricted than in previous years, particularly when compared to 2000–06 (fig. 24). The offshore spawning of mackerel, which is commonly regarded as being typical, occurred at very low densities in spring 2015 (figs. 23 and 24).

Conditions off central and southern California were unusually warm in spring 2015 (see elsewhere in this report). Mackerel eggs were found in water with surface temperatures of 14°–18°C. Sardine eggs are rarely found north of San Francisco in the spring, but in 2015 sardine spawned 445–556 km further north than usual (fig. 24). Sardine spawning centered near the California–Oregon border (41°–43°N) in a band about 90–110 km from shore in surface water temperatures of 12°–13°C (fig. 24). Egg densities off Oregon in spring 2015 were <1.5 eggs m^{-3}, which was extremely low compared to spring 2000–13 (fig. 24). There were also reports of sardine and anchovy spawning very close to shore off Newport, Oregon (R. Brodeur, NWFSC, personal communication), but inshore spawning was not detected by the SWFSC spring coastal pelagic fish survey.

During the summer 2014 CalCOFI cruise, dorado (*Coryphaena hippurus*) eggs were found in the continuous underway fish egg sampler (CUFES) samples in the southern part of the core area. Dorado apparently rarely spawn as far north as southern California—there

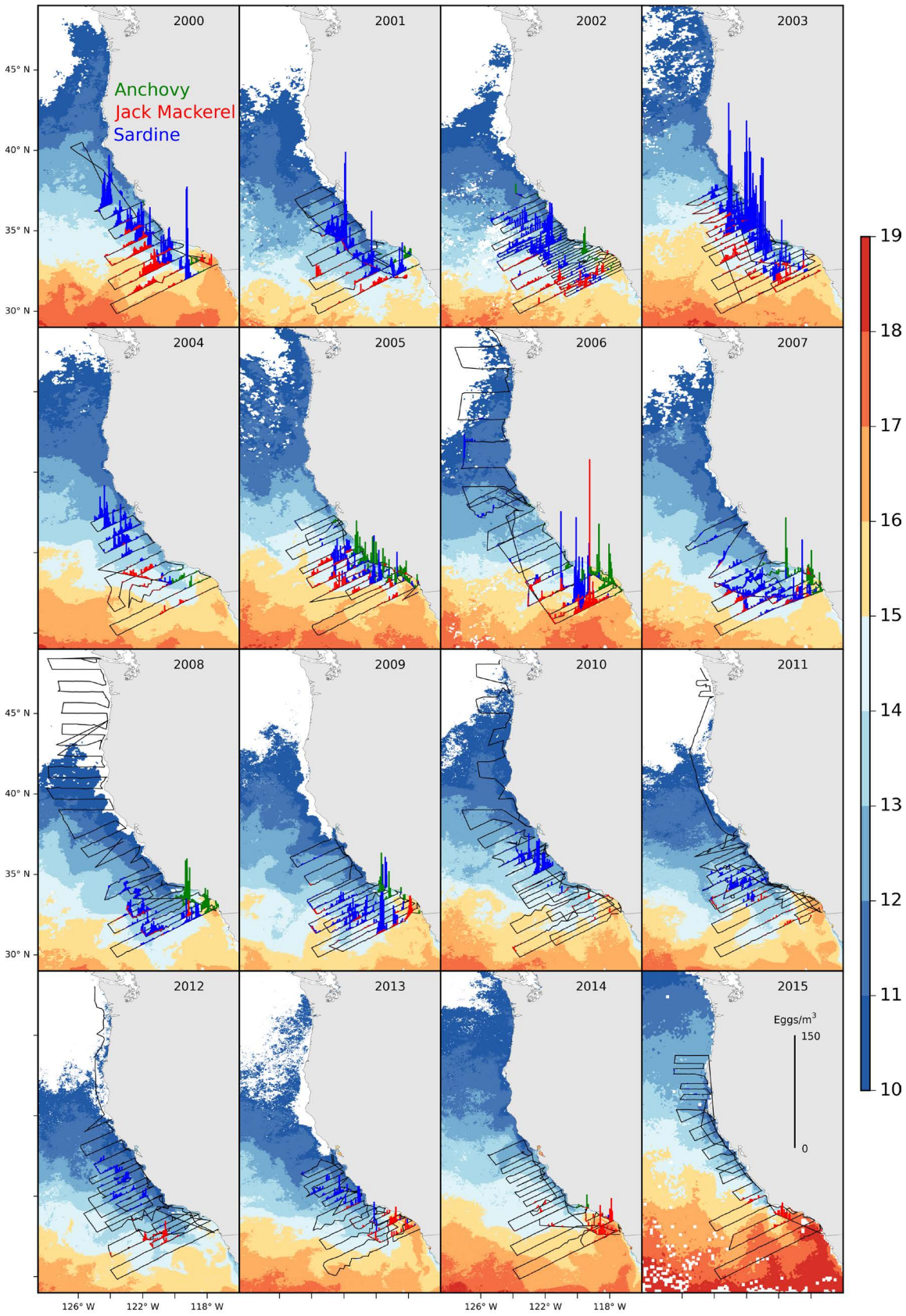

Figure 23. Density of eggs of sardine (blue), anchovy (green), and jack mackerel (red) collected with the continuous underway fish egg sampler (CUFES) overlaid on satellite sea surface temperatures (°C) derived from a monthly composite of April Pathfinder 5.5-km resolution (2000–08) or AVHRR 1.4 km resolution (2009–15) imagery. Ship track is shown by the black line.

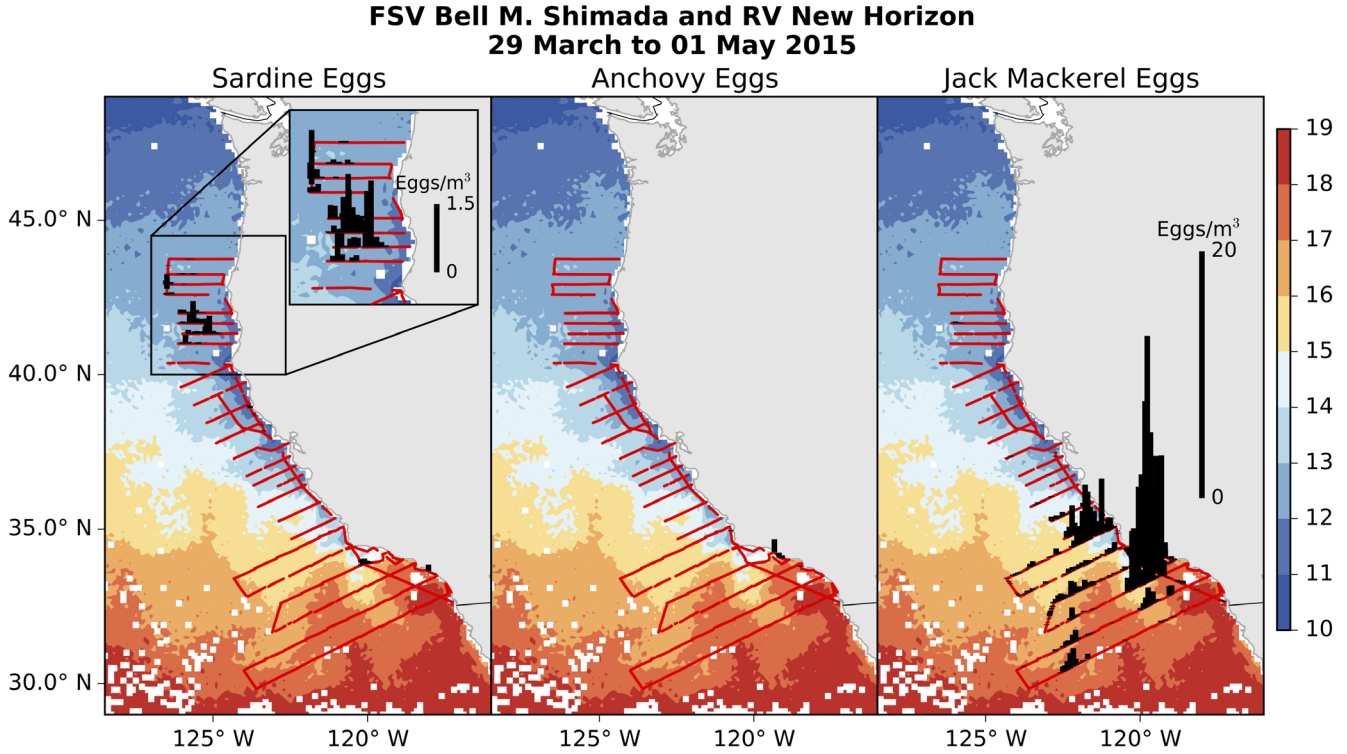

Figure 24. Density of eggs of sardine, anchovy, and jack mackerel collected with the continuous underway fish egg sampler (CUFES) during the spring 2015 CalCOFI and coastal pelagic fish cruises overlaid on satellite sea surface temperatures (°C).

are only two records north of the Mexican border since 1951 in the CalCOFI ichthyoplankton database—and spawning in the north during 2014 likely reflects the warm conditions at that time.

REGIONAL PATTERNS IN BIRDS AND MARINE MAMMALS

Common Murres at Yaquina Head, Oregon

Median hatch date for common murres at Yaquina Head in 2014 was 3 July, continuing the trend of later hatch dates beginning in 2010 (with a minor exception of 2012; fig. 25). Only 23% (+0.13 SE, 0.00–0.86 range) of the eggs laid hatched a chick (hatching success) and 17% (+0.11 SE, 0.00–0.81 range) of the eggs laid produced chicks that fledged (reproductive success; chicks > 15 days were considered fledged; fig. 25). Reproductive success in 2014 continued the trend of negative anomalies starting in 2011. Reproductive success in 2014 was the lowest recorded for this colony during 13 years of data collection, maintaining a 4 year run (2011–14) of low reproductive success that is less than half the success for the first four years of our study (2007–10, fig. 25). Only the reproductive success during the 1998 El Niño was slightly lower (Gladics et al. 2015).

Like the previous two seasons, much of the reproductive loss in 2014 was due to egg and chick preda-

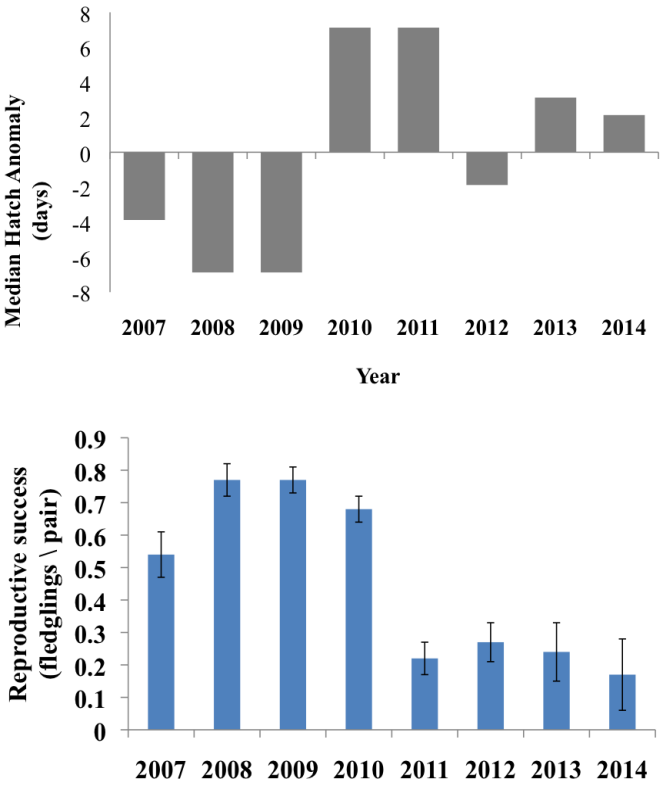

Figure 25. A) Median hatch date anomaly, and B) Reproductive success for common murres nesting at Yaquina Head, Oregon, 2007–14.

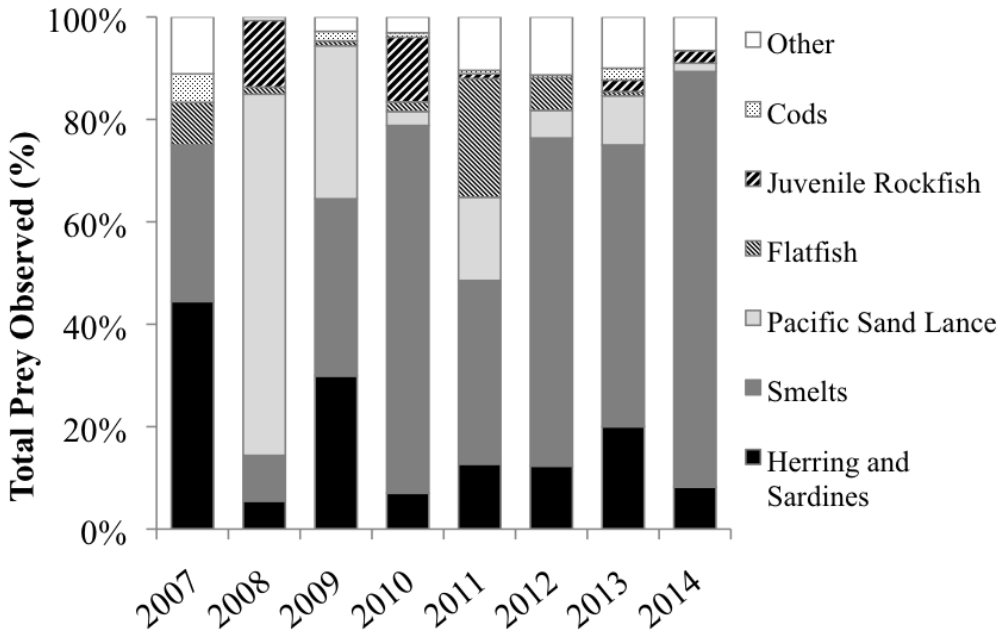

Figure 26. Prey fed to common murres chicks (% occurrence) at Yaquina Head Oregon, 2007–14.

tors. The total number of disturbances and the rate of murre egg and adult loss in 2014 was again high, similar to the previous four years. Disturbances and losses in 2010–14 were all 3–10 times higher than 2007–09. Disturbance rates first began to increase in 2010, and then greatly escalated during 2011–14 (Horton 2014). Bald eagles (*Haliaeetus leucocephalus*) were again the dominant disturbance source (49%, 36 of 75 disturbances). The frequent disturbances to a subcolony (flat top) resulted in total reproductive failure for those plots (reproductive success = 0.00 + 0.00 SE for 6 plots)—this was the first year that we observed complete failure of either subcolony. Unlike in 2012 when juvenile brown pelicans (*Pelecanus occidentalis*) resorted to eating fish regurgitated by murre chicks or eating murre chicks directly (Horton and Suryan 2012), there were no dramatic disturbances caused by pelicans in 2014, and pelicans were not observed landing on the colonies until the majority of murres had fledged.

Murre diets at Yaquina Head have varied annually. Forage fish species consumed in 2014 included primarily smelt (Osmeridae) and secondarily Pacific herring or sardine (Clupeidae; fig. 26). A notable difference in diets in recent years has been the dominance of smelt since 2010 (with minor exception of 2011). Prior to this period, annual diet composition varied annually between dominance of smelt, Pacific sand lance (*Ammodytes hexapterus*), and clupeids, or occasionally relatively equal proportions of each in a given year (fig. 26). The lack of sand lance and clupeids since 2010 continued and was especially prominent in 2014. Sand lance are generally more prominent in cold water years (Gladics et al. 2014, 2015), as highlighted by their prevalence in 2008 (fig. 26). Clupeids (primarily Pacific herring, *Clupea pallasii*), are generally associated with warmer water and positive PDO (Gladics et al. 2015).

Summary of Common Murre Reproductive Success, Phenology, and Diet at Castle Rock National Wildlife Refuge: 2007–14

Castle Rock National Wildlife Refuge (hereafter Castle Rock) is the most populous single-island seabird breeding colony in California. Located in the northern California Current system, this island is off the coast of Crescent City, just south of Point St. George. To facilitate long-term monitoring of seabirds nesting at this colony, a remotely-controlled video monitoring system was installed at this island in 2006. For purposes of assessing the state of the California Current, the reproductive performance of common murre and Brandt's cormorants is provided. For common murre, the composition of prey delivered to chicks between 2007 and 2014 is also provided.

Common murre are the most abundant surface-nesting seabird at Castle Rock and their reproductive success, nesting phenology, and chick diet have been studied since 2007. The percent of nesting pairs that successfully fledged young in 2014 was based on 81 nest-sites that were monitored every other day for the entire breeding season. During 2014, 83% of nests fledged young, which was 10% greater than the long-term average for this colony (fig. 27). Although murres do not reflect upwelling directly, the increased availability of food associated with upwelling improves the body condition of egg-laying

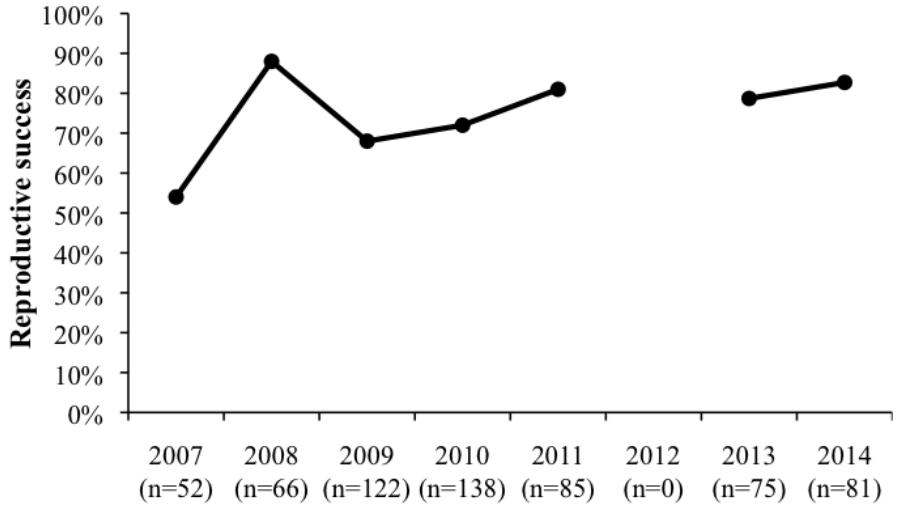

Figure 27. Percent of common murre (*Uria aalge*) nesting pairs that successfully fledged young between 2007 and 2014 at Castle Rock National Wildlife Refuge, Del Norte County, CA. The sample size (n) represents the total number of nesting pairs observed per year, and this figure does not include the success of replacement clutches. Reproductive success could not be determined in 2012 due to early failure of the video monitoring system.

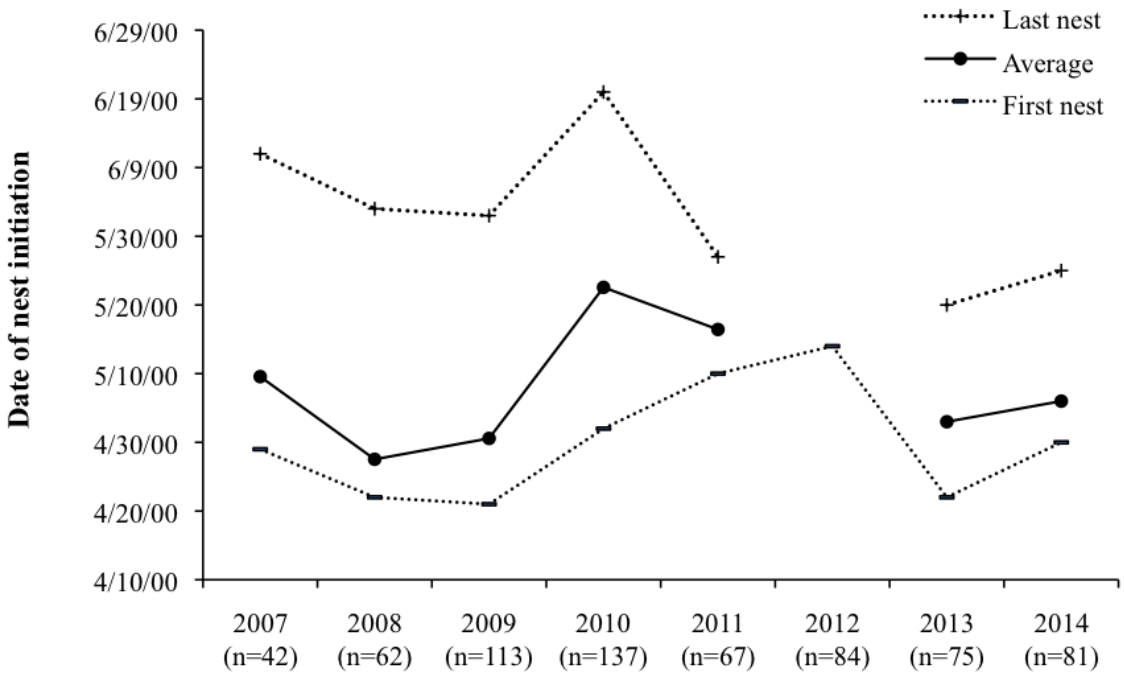

Figure 28. First, average, and last dates for nests initiated by common murres between 2007 and 2014 at Castle Rock National Wildlife Refuge, Del Norte County, CA. The date of nest initiation was the defined as the day that an egg was laid at a nest site. The sample size (n) represents the total number of nests observed each year where nest initiation dates were accurate to ±3.5 days. The average and last date of nest initiation could not be determined in 2012 due to early failure of the video monitoring system.

females and thereby influences the timing of nesting (Perrins 1970; Reed et al. 2006; Schroeder et al. 2009). In 2014, the average nest initiation date was 6 May, which is 2 days earlier than the long-term average observed at this colony (fig. 28). To determine prey composition, 2-hour diet surveys were conducted 6 days per week during the murre chick-rearing period (approximately 70 hours surveyed in 2014). In 2013, a total of 12 prey types were identified and all prey types had been observed in previous years. Prey composition was generally similar to other years, with smelt (*Osmeridae*) being the predominant prey fed to chicks and rockfish being the second most common prey fed to chicks (fig. 29). Unlike other years, California Market Squid (*Loligo opalescence*) observations were 2.2 times more frequent and was the third most common prey type fed to chicks in 2014.

Brandt's cormorant are the second-most abundant surface-nesting seabird at Castle Rock and their repro-

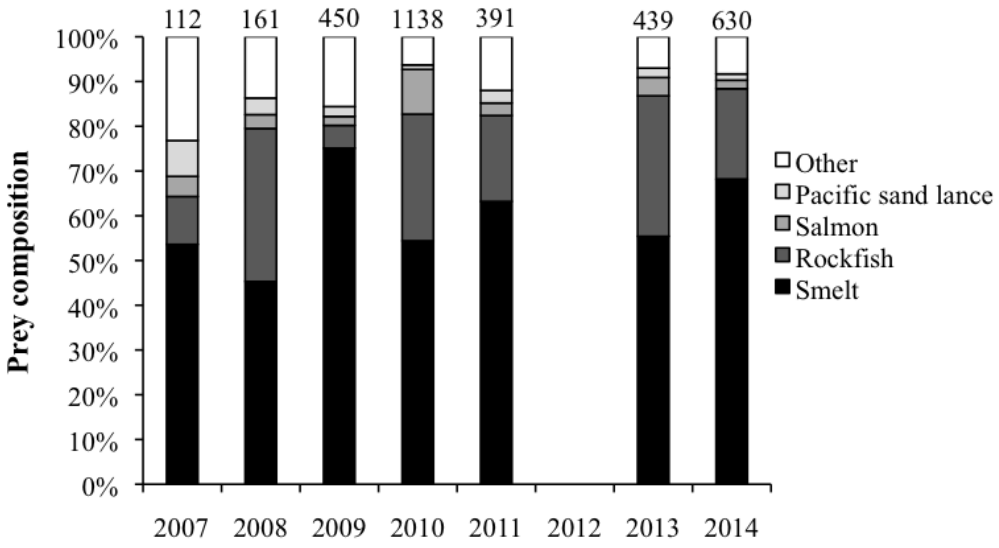

Figure 29. Composition of prey delivered to chicks by common murre between 2007 and 2014 at Castle Rock National Wildlife Refuge, Del Norte County, CA. Numbers above each bar indicate the total number of prey identified each year. Prey composition could not be determined in 2012 due to early failure of the video monitoring system.

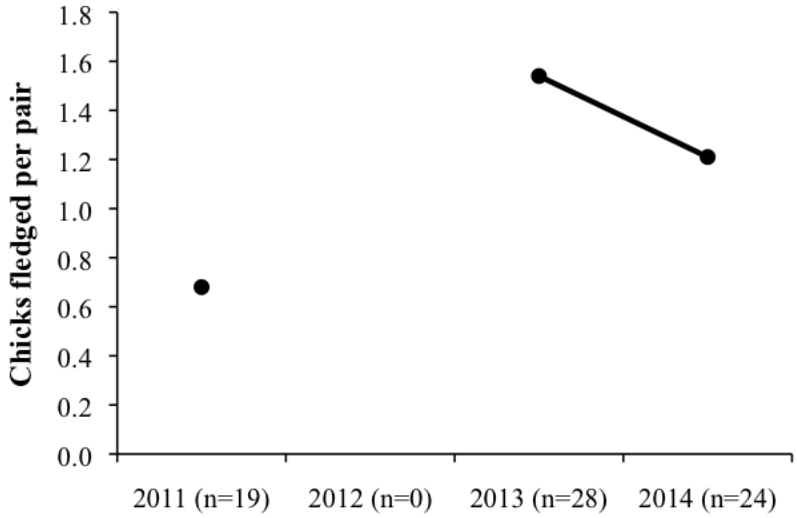

Figure 30. Chicks fledged per nesting pair of Brandt's cormorant (*Phalacrocorax penicillatus*) between 2007 and 2014 at Castle Rock National Wildlife Refuge, Del Norte County, CA. The sample size (n) represents the total number of nesting pairs observed per year, and this figure does not include the success of replacement clutches. Reproductive success could not be determined in 2012 due to early failure of the video monitoring system.

ductive success has been studied since 2011. The reproductive success of Brandt's cormorants, measured as the number of fledglings produced per pair, was determined by monitoring 24 nests every four days for the entire breeding season. In 2014, breeding pairs produced 1.21 chicks on average, which was 43% greater than the year with the poorest reproduction (2011) and 27% less than the year with the most successful reproduction (2013; fig. 30).

Breeding Success of Seabirds at Southeast Farallon Island

The 2014 seabird breeding season at Southeast Farallon Island (SEFI), California was a mixed year with higher breeding populations and increased productivity for some species while declines were observed for others (fig. 31). Reproductive success of the planktivorous Cassin's auklets (*Ptychoramphus aleuticus*), though lower than the previous four years, continued to be exceptionally high relative to the long-term mean for this colony. The fledging success for first broods was the highest observed in the time series, as Cassin's were again able to take advantage of high zooplankton production during the early part of the breeding season. However, Cassin's auklets were unable to successfully fledge any second broods for the first time since 2008, leading to the overall productivity decline observed this year. In contrast, piscivorous species including pigeon

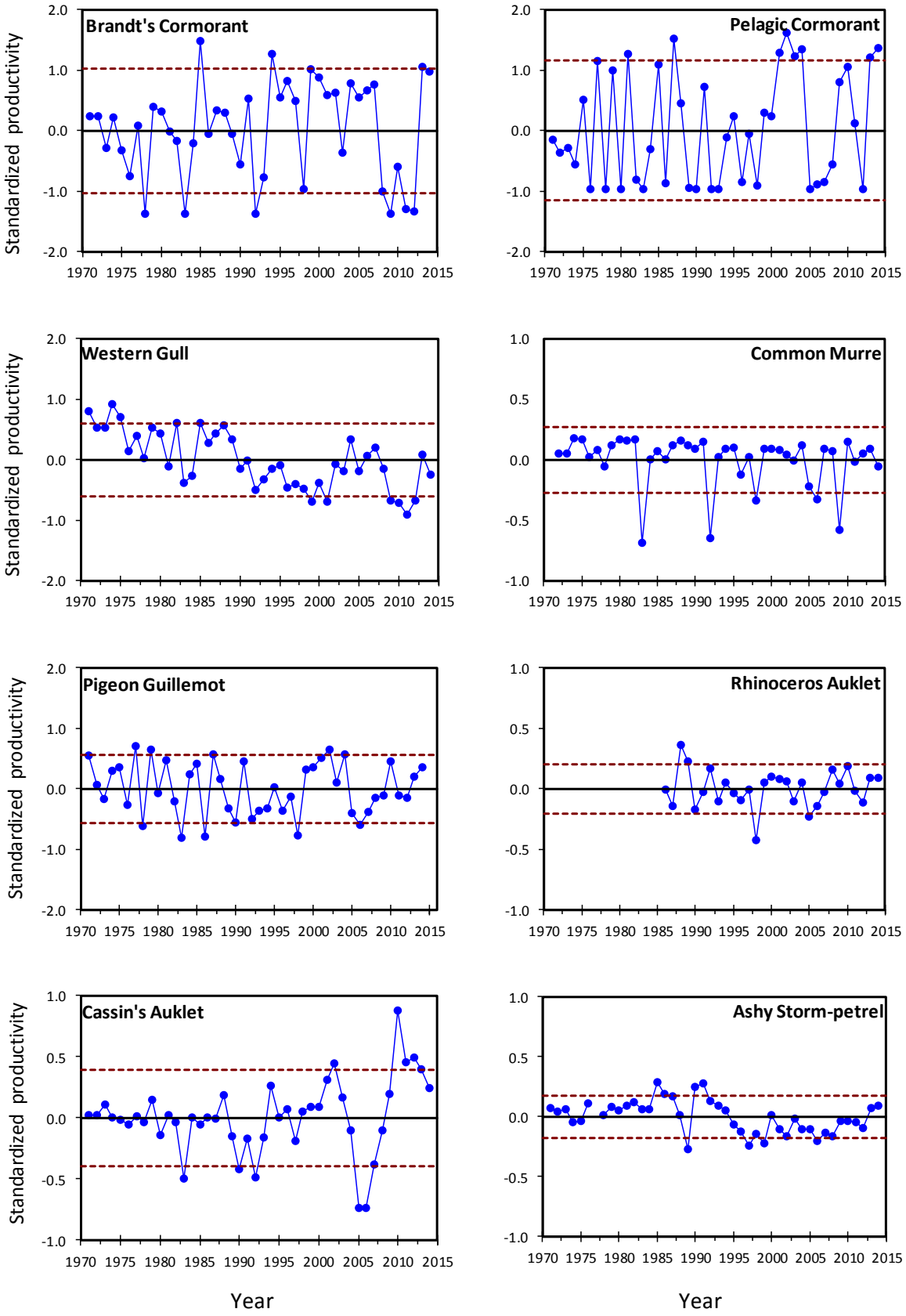

Figure 31. Standardized productivity anomalies (annual productivity—long term mean) for 8 species of seabirds on SEFI, 1971–2014. The dashed lines represent the 80% confidence interval for the long-term mean.

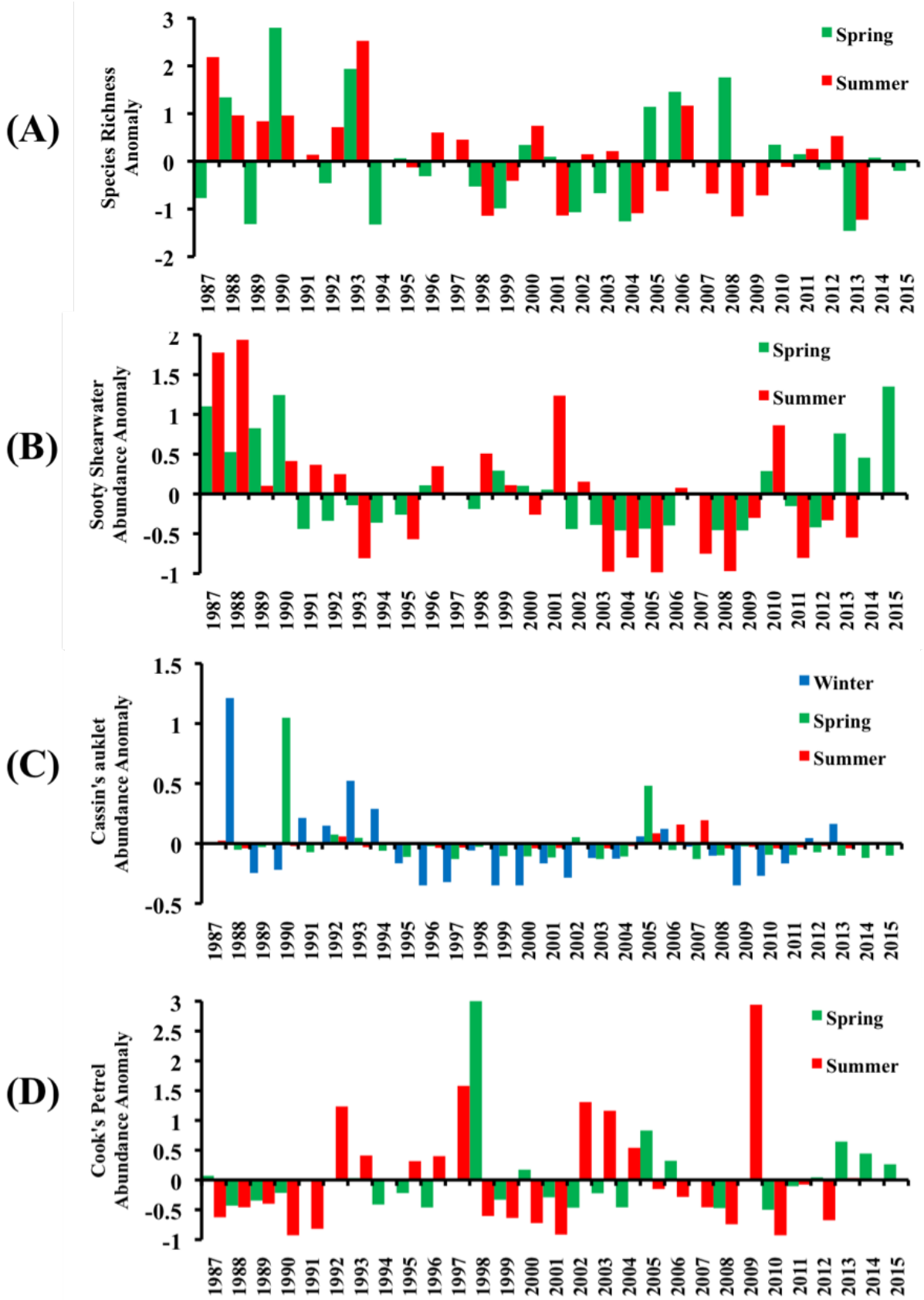

Figure 32. Patterns of change in the abundance (expressed as anomaly of log density; long-term mean subtracted) of (a) seabird species richness, (b) sooty shearwater (*Puffinus griesus*), (c) Cassin's auklet (*Ptychoramphus aleuticus*), and (d) Cook's petrel (*Pterodroma cookii*).

guillemots (*Cepphus columba*), rhinoceros auklets (*Cerorhinca monocerata*), Brandt's cormorants (*Phalacrocorax penicillatus*) and Pelagic cormorants (*Phalacrocorax pelagicus*) exhibited higher reproductive success relative to last season and well above the long-term mean (fig. 31). Success for these species was likely driven by a high abundance of juvenile rockfish available throughout the early and middle parts of the season. Common murres (*Uria aalge*), though also benefiting from high rockfish abundance to achieve exceptionally high fledging success, exhibited lower than average reproductive success due to an unusually high rate of egg failure. During mid-July, ocean conditions deteriorated, with a rapid increase in sea surface temperature and a corresponding reduction in prey availability leading to poor success for later breeding individuals of all species and the failure of second broods for Cassin's auklets. Anchovies and other larger forage fishes continued to be largely absent from seabird diet, but it would appear that the birds were able to compensate this season with other prey items.

Seabirds in the CalCOFI Region

As part of CalCOFI, now supplemented by the CCE-LTER and SCCOOS programs, data on seasonal seabird distribution and abundance has been collected since spring 1987. Seabird distribution and abundance derived from CalCOFI surveys have indicated several important aspects regarding the biological conditions of the southern California Current, including: long-term declines in seabird abundance and species richness related to ocean climate and forage fish availability (Veit et al. 1996; Hyrenbach and Veit 2003; Sydeman et al. 2009, 2015; Santora and Sydeman 2015), as well as the presence and persistence of biological "hotspots" (Yen et al. 2006; Santora and Sydeman 2015). As examples of long-term variability of seabird abundance (ln anomaly density, expressed as numbers km^{-2}), we present data up to spring 2015 on seabird species richness (number of species observed per survey) as well as sooty shearwater (*Puffinus griseus*), Cassin's auklet (*Ptychoramphus aleuticus*) and Cook's petrel (*Pterodroma cookii*) abundance as "cold-water" (shearwater and auklet) and "warm-water" (petrel) indicators.

Seabird species richness (fig. 32A) has exhibited a long-term decline in the CalCOFI region, and has been negative since 2013. The decline in species richness possibly indicates that biophysical changes occurring in the southern California Current is impacting the overall at-sea avifauna. Hyrenbach and Veit (2003) suggested that species with warm-water affinities increased during warm ocean conditions, while those with cold-water affinities decreased. Sooty shearwaters (fig. 32B), a species with cold-water affinities, are southern hemisphere migrants and are most abundant in coastal waters of the California Current during the spring and summer. Shearwater density during spring has declined since surveys began in 1987, with each successive peak in abundance (i.e., 1990, 2001, and 2010) lower than the preceding one. However, shearwaters have shown strong consecutive positive anomalies since spring 2013, with spring 2015 being the highest anomaly since 1990; this is surprising given the warm-water conditions that have persisted off southern California since 2014. Further research is needed to examine why shearwaters have increased in number and what the mechanism(s) may be for their recent influx to the CalCOFI region (i.e., poor breeding leading to abandonment of colonies during 2013–14). Cassin's auklets (fig. 32C) are resident in the California Current year-round, but are most abundant in the CalCOFI region in winter. After exhibiting a positive anomaly in winter 2013, the anomaly of auklet abundance has been close to zero, suggesting that auklets have not undergone any major redistribution patterns during winter. Cook's petrels (fig. 32D) are southern hemisphere migrants and generally occur in hotspots associated with subtropical waters within the western edge of the CalCOFI grid (Santora and Sydeman 2015). Strong peaks in Cook's petrel anomalies, usually during summer surveys, are generally associated with El Niño years. Recent spring surveys indicate moderate positive anomalies of Cook's petrel and it's anticipated that given the recent warm ocean conditions off southern California, that this species should show a strong positive anomaly in summer 2015.

California Sea Lions at San Miguel Island, California

California sea lions (*Zalophus californianus*) are permanent residents of the CCS, breeding in the California Channel Islands and feeding throughout the CCS in coastal and offshore habitats. They are also sensitive to changes in the CCS on different temporal and spatial scales and so provide a good indicator species for the status of the CCS at the upper trophic level (Melin et al. 2012). Two indices are particularly sensitive measures of prey availability to California sea lions, pup production, and pup growth during the period of nutritional dependence. Pup production is a result of successful pregnancies and is an indicator of prey availability to and nutritional status of adult females from October to the following June. Pup growth from birth to 7 months of age is an index of the transfer of energy from the mother to the pup through lactation between June and the following February, which is related to prey availability to adult females during that time.

At San Miguel Island, successful pup births, as measured by counts of live pups, in 2014 were 11% higher

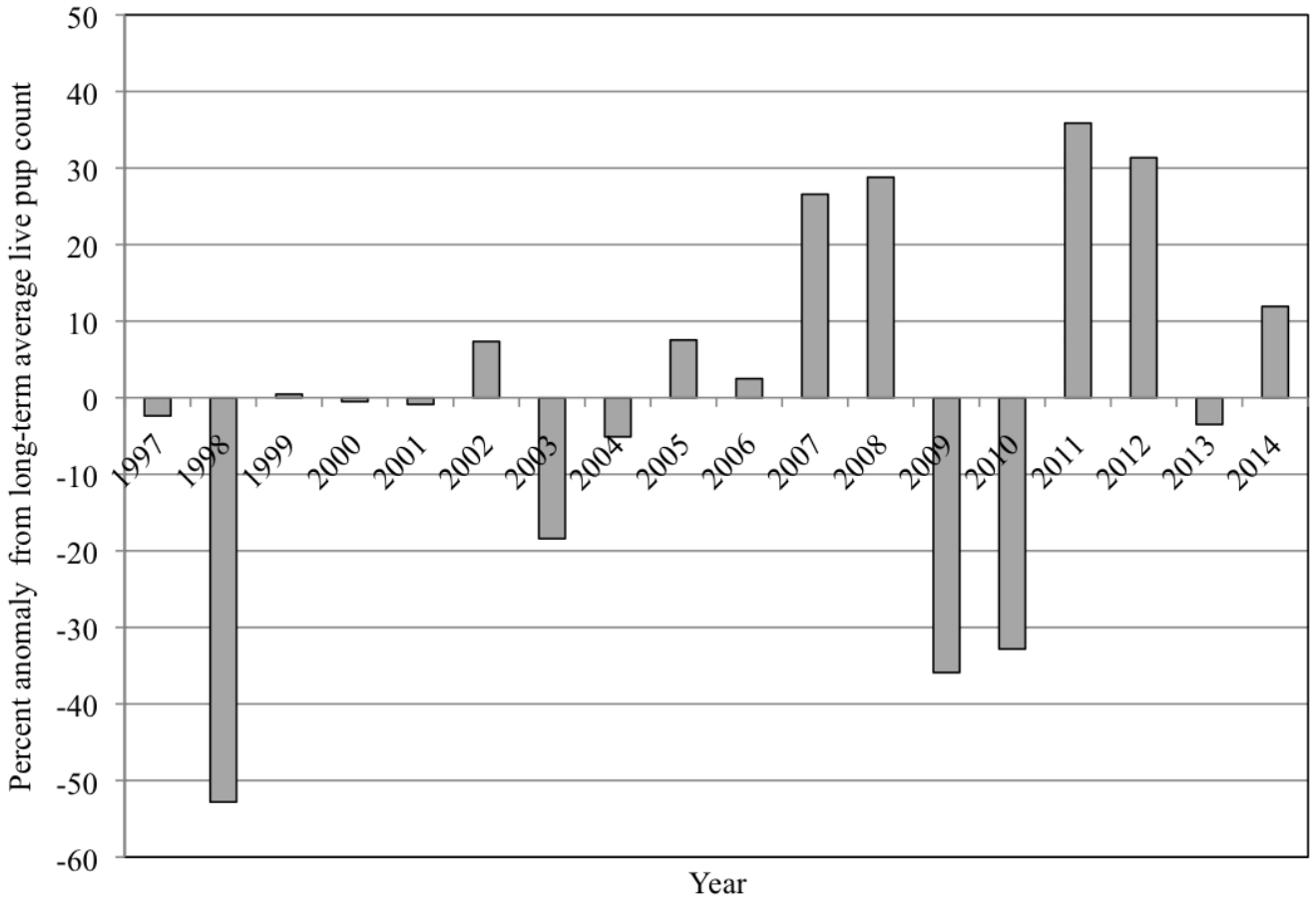

Figure 33. The percent anomaly of live California sea lion pup counts at San Miguel Island, California, based on a long-term average of live pup counts between 1997–2014 in late July when surviving pups were about 6 weeks old.

than the long-term average between 1997 and 2014 (fig. 33). However, similar to previous years, pup condition and pup growth was poor for the 2014 cohort. The average weight of three-month-old pups were 17% and 20% lower than the long-term average for female and male pups, respectively (fig. 34). Growth rates from three to seven months old were 78% below normal for both sexes and similar to the 2012 cohort (fig. 35).

For the past five of six years, the California sea lion population has experienced low pup survival, low pup births or both (Melin et al. 2010; Melin et al. 2012; Leising et al. 2014). An unusual mortality event (UME) was declared for California sea lions in southern California (http://www.nmfs.noaa.gov/pr/health/mmume/californiasealions2013.htm) in response to unprecedented numbers of young pups from the 2012 and 2014 cohorts stranding along the coast between January and April and poor condition of pups at San Miguel Island and other rookeries during the winter (Wells et al. 2013; Leising et al. 2014). The two cohorts experienced dramatically different ocean conditions. During winter 2013, ocean conditions were unusually cold and had high primary productivity (Wells et al. 2013) and should have produced good foraging conditions for nursing females. In contrast, ocean conditions during the winter 2014 were unusually warm due to the continuation of a positive signal in the Pacific Decadal Oscillation and the presence of anomalously large warm water pools along the West Coast. Fisheries surveys during the springs in both years indicated that several of the primary fish prey of California sea lions including Pacific sardine (*Sardinops sagax*), northern anchovy (*Engraulis mordax*), and Pacific hake (*Merluccius productus*) were not abundant along the central California coast in the foraging range of nursing females (Bjorkstedt et al. 2012; Wells et al. 2013; Leising et al. 2014: this volume). Analysis of scat contents of California sea lion females during these periods indicated increased consumption of rockfish (*Sebastes* spp.) and market squid (*Doryteuthis opalescens*) (Melin et al. in Review). Thus, the composition of the prey community available to nursing females was similar in 2012 and 2014 but quite different from previous years when pups were in better condition (Melin et al. 2012). Consequently, the current hypothesis for the poor condition of dependent pups and ultimately, large numbers of weaned pups stranding on the coasts is that alterations in

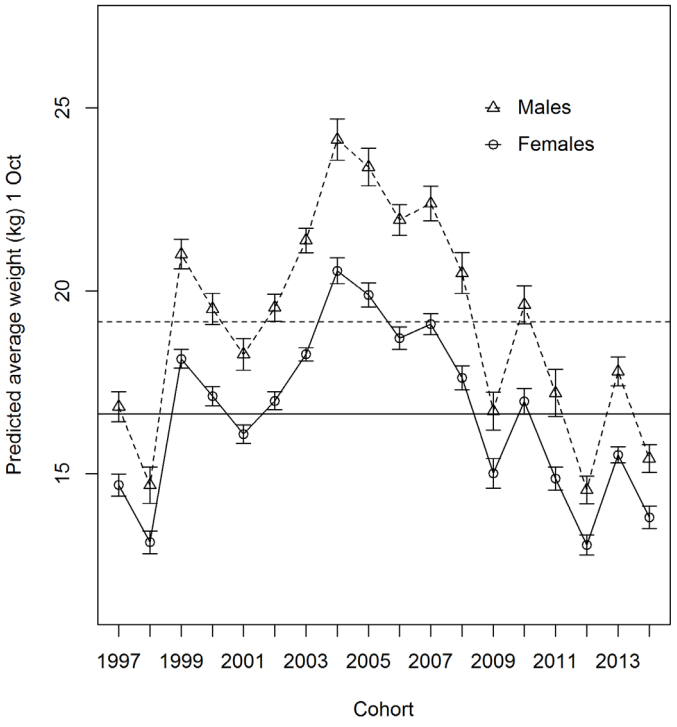

Figure 34. Predicted average weights of 3-month-old female (open circle) and male (open triangle) California sea lion pups at San Miguel Island, California, 1997–2014 and long-term average between 1975 and 2014 for females (solid line) and males (dashed line). Error bars are ± 1 standard error.

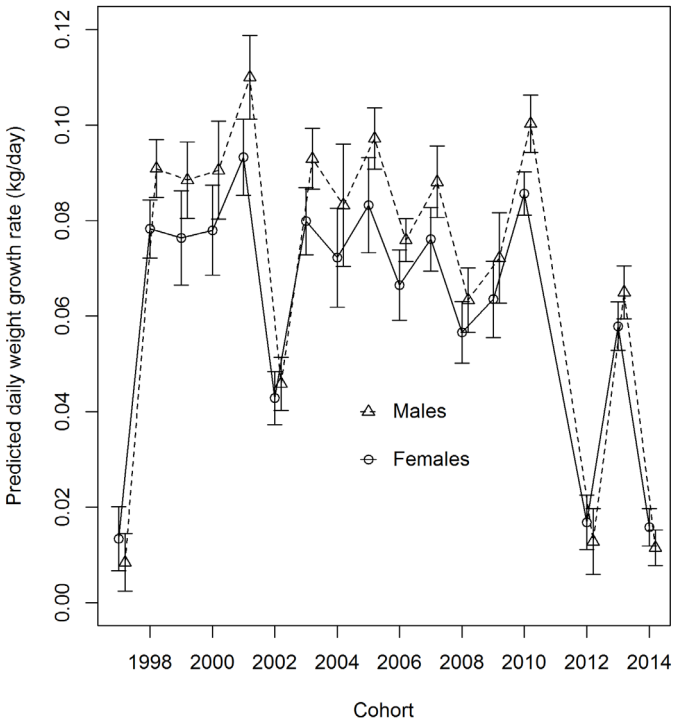

Figure 35. Predicted average daily growth rate of female (open circle) and male (open triangle) California sea lion pups between 4 and 7 months old at San Miguel Island, California, 1997–2014. Error bars are ±1 standard error.

the prey community due to oceanographic changes on local and regional scales have resulted in nursing females being unable to fully support lactation and the needs of their dependent pups. We anticipate this trend to continue until the diversity and abundance of the prey community increases and provides greater nutritional value to nursing females.

DISCUSSION

The winter of 2013–14 saw a drastic change in the conditions throughout the California Current as compared to the previous years (2013 being a record-breaking year of high cumulative upwelling; Wells et al. 2013; Leising et al. 2014). Between fall of 2013 and spring of 2014, the PDO switched sign to positive, indicating warming coastal waters, the NPGO switched sign to negative, typically indicating lower productivity in the southern CCS, and the MEI switched sign to positive, indicating the possible development of an El Niño. During 2014, these trends continued, along with increasingly warm waters throughout the CCS. During spring 2015, there was some moderate cooling along the central and northern coast within the CCS, due to upwelling. Meanwhile, surface waters along the eastern equatorial Pacific continued to warm during mid-2015, leading to high values of the MEI, suggesting potentially the strongest El Niño since 1997–98, with impacts likely reaching the CCS during winter 2015–16. Preceding the development of the El Niño, the fall of 2013 in the NE Pacific saw a rise of sea surface temperatures, likely due to a shift in wind patterns, a lack of winter storms, and an increase in sea level pressure (Bond et al. 2015); this large area of high SST anomaly was labeled the blob by Bond. There was also a rise in sea surface temperatures both coastally and offshore of southern California (distinct from the main portion of the blob in the NE Pacific) in mid-2014, also most likely related to changes in wind patterns (detailed below). Typical atmospheric patterns over the NE Pacific were replaced by a resilient ridge of high pressure, which greatly altered the ocean surface structure, and continues to do so as of the writing of this report. The result has been a continued warming of surface waters in the NE Pacific, at times in excess of 4°C above the climatological mean.

Warming in the Southern CCS

The Southern California Warm Anomaly (SCWA; as distinct geographically from the blob in the NE Pacific) was first evident in the spring of 2014 as a band of warm surface water along the shelf break (fig. 36). It is unlikely that this feature advected into the region from the north since the CC was located at this time in the offshore areas of the domain (west of Station 80). During the summer this feature intensified, but its spatial footprint

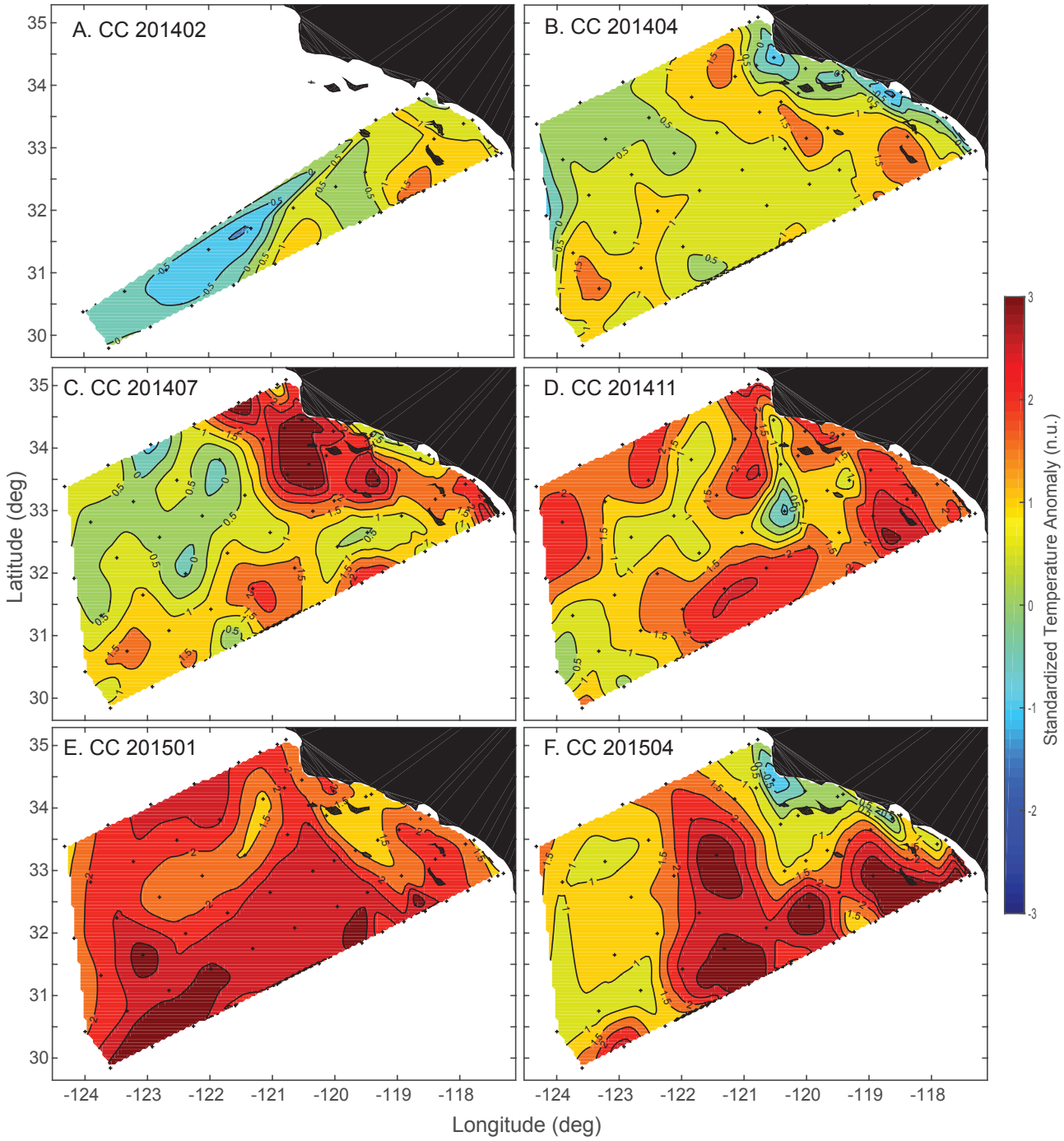

Figure 36. Temperature anomalies at a depth of 10 m standardized by the standard deviation of temperature for the CalCOFI 66 station standard grid for the last six CalCOFI cruises that covered the 2014–15 warm anomaly, i.e., the winter (A), spring (B), summer (C), and fall (D) of 2014 and the winter (E) and spring (F) of 2015. The 2014 winter cruise was not completed due to ship failure.

did not. Warm surface layer anomalies off Pt. Conception during the summer of 2014 were partly driven by extremely low rates of coastal upwelling (fig. 2); i.e., no cold water was brought into the surface layer as usually happens during this time of the year. During the fall of 2014 and winter of 2015 these 10 m anomalies intensified, covering the complete CalCOFI domain (fig. 36).

One way to place these events in context is to examine long-term data in the region to look for comparisons. Subsurface temperature data have been collected along line 90 of the CalCOFI grid since 1950. Annual temperature anomalies at a depth of 10 m along this line for the time period 1984 to 2015 (fig. 37A) are highly correlated with the temperature anomalies of the

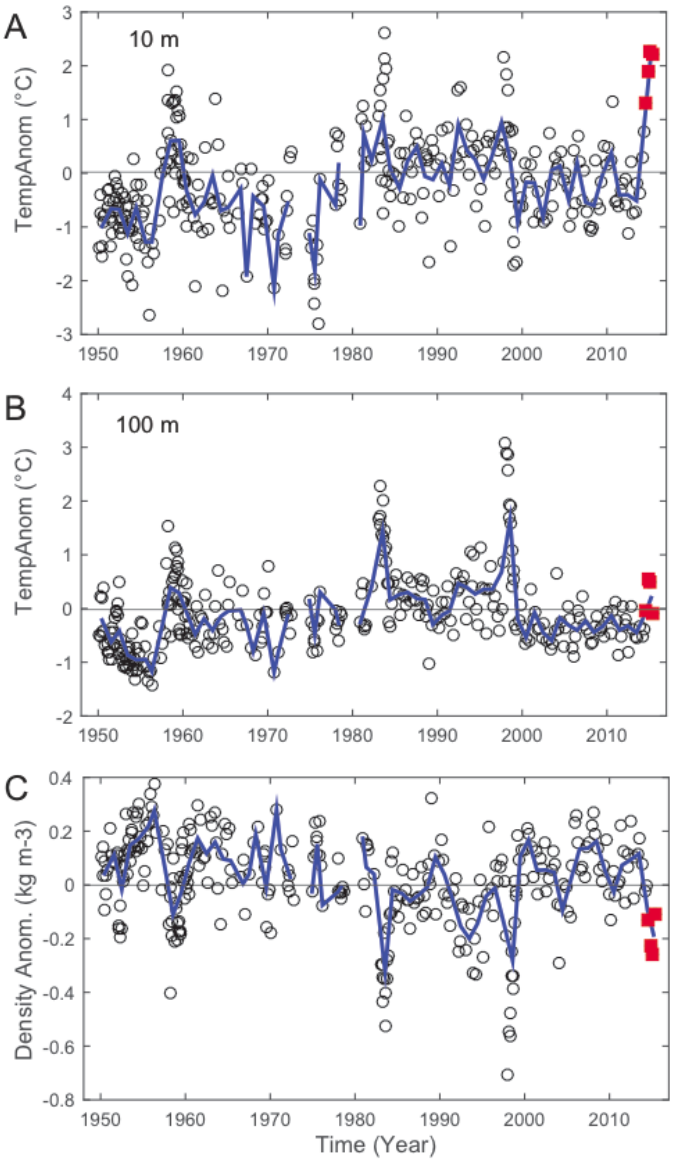

Figure 37. Cruise averages of property anomalies for CalCOFI Line 90, stations 30 to 90 for the time period 1950 to 2015. A) temperature anomaly at 10 m, B) temperature anomaly at 100 m, and C) density anomaly at 100 m. Data are derived and plotted as described for Figure 11.

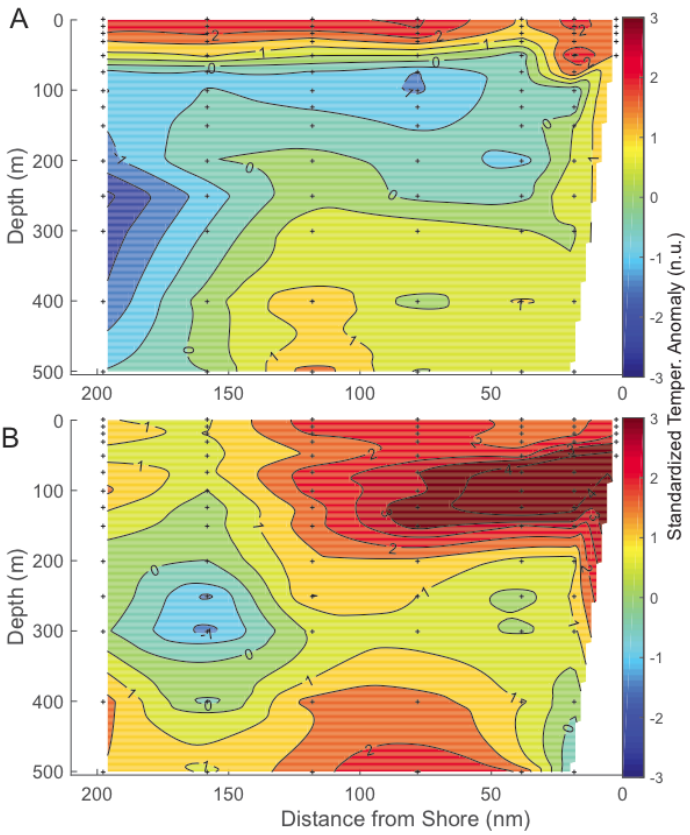

Figure 38. Standardized temperature anomalies, these have no units (n.u.), along CalCOFI line 80 plotted against depth and distance from shore for periods corresponding to the height of the 2014–15 warm anomaly (A: CC201501) and the 1998 El Niño (B: CC199802). Plotted data are deviations from expected values in terms of standard deviations in order to illustrate the strength of the relative changes at different depths.

entire CalCOFI domain (rho = 0.92, $p < 0.001$). These data show that the recent anomalies at a depth of 10 m were as large as those observed during the strong El Niños of 1957–58, 1982–83, and 1997–98 (fig. 37A). Temperature anomalies at a depth of 100 m observed during the El Niños and the SCWA differ dramatically: whereas relative anomalies during the El Niños were stronger at 100 m compared to the surface layer, anomalies at a depth of 100 m during the SCWA were slightly elevated only during the fall of 2014 and the winter of 2015. Consistent with these differences, dramatically different distributions of temperature with depth and distance from shore were observed throughout the CalCOFI domain during the winters of 1998 and 2015 (e.g., Line 80, fig. 38). The strongly positive relative temperature anomalies of 2015 extended to the far offshore but were confined to the surface layer (upper ~50 m). In contrast, the relative anomalies of 1998 were strongest at depth of 50 to 150 m and did not extend offshore (fig. 38). These patterns suggest that the coastal subsurface advective component that drives water column properties during El Niños was not active during the SCWA. Increasing transport, temperature, and salinity of the California Undercurrent (CU) are important drivers of changing water mass characteristics during El Niños (Lynn and Bograd 2002). Such changes in water mass characteristics are clearly evident in the core of the CU (CalCOFI station 90.30, depth 200 to 300 m) during the strong El Niños of 1982–83 and 97–98; (e.g., spiciness, fig. 39). Interestingly, strongly positive spiciness anomalies were only observed during the summer of 2014 and not during any other time period corresponding to the SCWA.

Properties at the σ_t 26.4 isopycnal (fig. S6), which is found at a depth of about 200 m in the CalCOFI

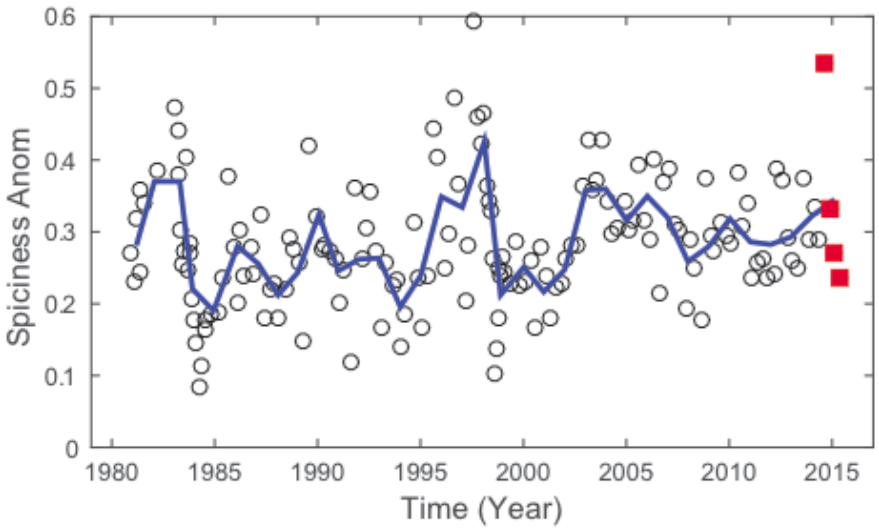

Figure 39. Cruise averages of spiciness at a depth of 200 to 300 m at Station 90.30 for the time period 1981 to 2015. The core of the California Undercurrent is usually found in this location. Data are derived and plotted as described for Figure 11.

domain, also did not change in synchrony with the SCWA. The depth of this isopycnal increased by about 20 m during this time (fig. S6A), with values slightly less than those observed during the 1997–98 El Niño. Properties on this isopycnal have been used in the past as indicators of long-term changes of southern California Current deep waters (e.g., Bjorkstedt et al. 2011, 2012; Bograd et al. 2014). The decline of oxygen concentrations between the years 2000 and 2012, and the concomitant increase of NO_3 (fig. S6), was assumed to be driven by basin-wide drivers (Bjorkstedt et al. 2012). The dramatic reversal of the oxygen and nitrate trends over the last 3 years forces us to rethink this assumption. The drivers of these recent changes are unclear at the present.

The potential drivers of the SCWA are local warming of the surface layer due to atmospheric anomalies, the advection of anomalously warm surface waters into the region from the North Pacific blob, and Kelvin waves travelling up the coast driven by equatorial anomalies. The above analysis of the waters of the California Undercurrent suggests that waters of equatorial origin may have been present in the region during the summer of 2014 but not during other periods of time. The absence of positive temperature anomalies close to the coast at depths of 50 to 150 m during the SCWA supports the conclusion that equatorial forcing of the region was weak or negligible during this time. Further supporting this conclusion are the observations from the IMECOCAL, Baja, California region. As noted above, although surface waters when averaged across the IMECOCAL survey were warm and salty as compared to the long-term mean, these anomalies were confined to the surface, and there was no northward flow north of Punta Eugenia, as has occurred in the past during warm events such as El Niño (Durazo 2015). The strongly positive surface layer anomalies observed during the summer of 2014 within the CalCOFI region were in part driven by weak coastal winds, i.e., weak coastal upwelling not injecting cold subsurface water into the mixed layer and weak wind-induced mixing, resulting in shallow and extremely warm mixed layers. Exact identification of the drivers of the SCWA off southern California is limited by the low temporal resolution of the CalCOFI time series. An analysis of high-resolution sampling via gliders may offer a way to more explicitly address this, but is beyond the scope of this report.

Warming Throughout the CCS

Examining the timing of warming along the entire current, and comparing with the evolution of the strong El Niño of 1997–98 may help with interpreting which forces dominated within the different segments of the CCS. As noted in Bond et al. (2015), the anomalous warm blob began offshore in the Gulf of Alaska in late 2013, but began to be seen in the coastal region as early as May of 2014 off of British Columbia. The exact timing of the onset of warming throughout the CCS can be seen by examining the anomaly of remotely sensed SST data (fig. 40, left-hand panels) in the offshore region, and buoy SST temperatures from the nearshore region (fig. 40, right-hand panels). For the more-offshore locations (by approximately 1°–2° compared to the nearby buoys) examined using remotely sensed data, warming during mid-2014 to mid-2015 was very similar in magnitude to that seen during 1997–98 (between 2°–4°C positive anomaly depending on location). However, the warming that occurred during this period was not due directly to El Niño, which had only begun to warm

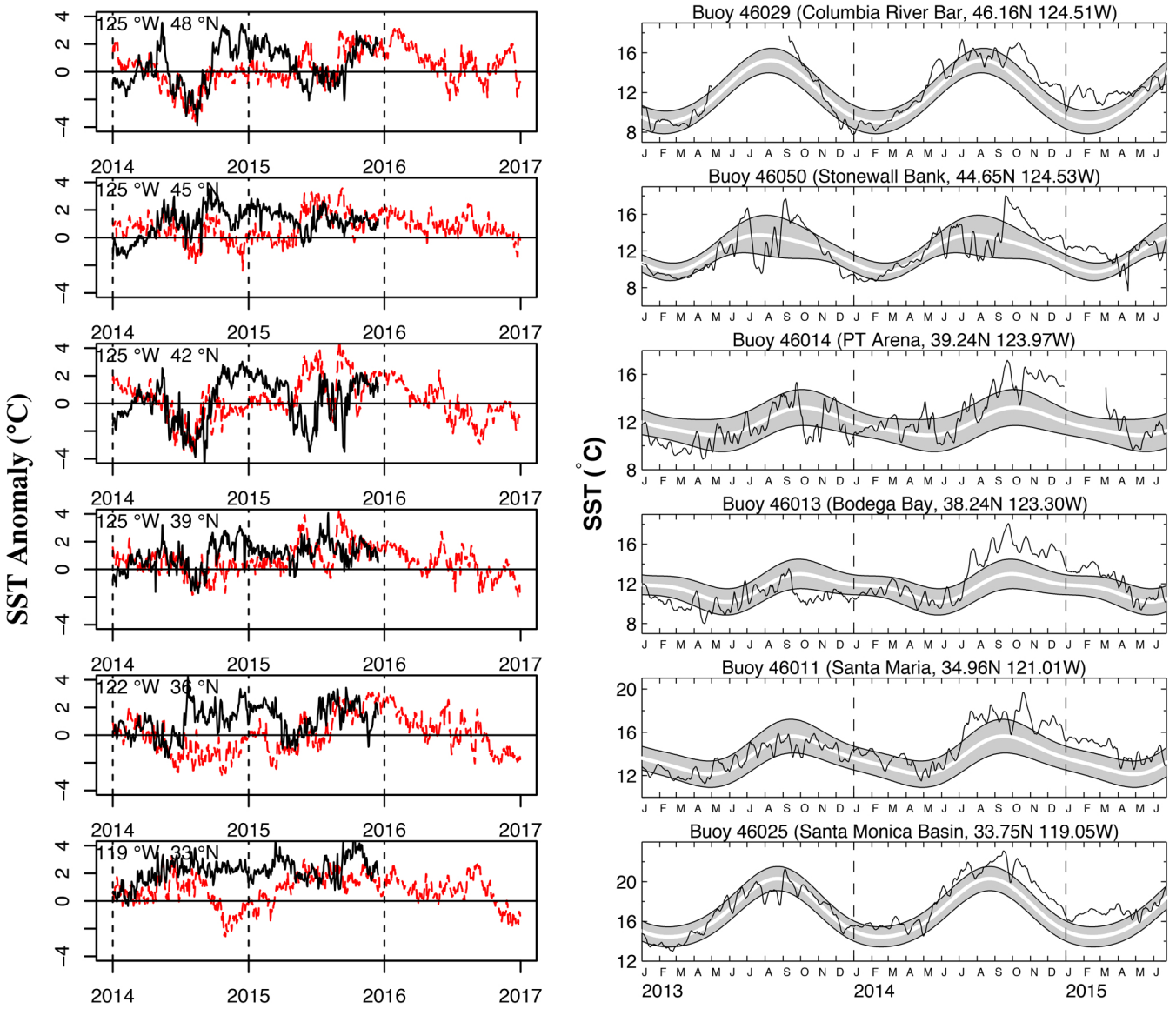

Figure 40. Daily sea surface temperature (SST) anomalies (left-hand panels) for selected locations along the US West Coast (locations same as those calculated for upwelling indices in Figure 3; data from the Daily Optimum Interpolation AVHRR data set, see http://coastwatch.pfeg.noaa.gov/erddap/griddap/ncdcOisst2Agg.html) with black line indicating 2014–15, and red line indicating 1996–98, and (right-hand panels) SST from selected buoys along the US West Coast, with grey region indicating the range of climatological values, white line the climatological mean, and black line the current (2013–15) values.

the equatorial Niño 3.4 region during mid-2014, leaving insufficient time for propagating Kelvin waves to reach even the southern portions of the CCS. Off British Columbia, anomalous warming occurred as early as May 2014, but then the water cooled, most likely due to increased upwelling, as suggested by the upwelling index for this time and location (fig. 40, top left, and fig. 2). Warmer conditions then returned very rapidly after the cessation of upwelling in September. Except for the most southerly Southern California Bight location (fig. 40, lower left panel, 33°N), the other more-offshore locations examined followed a similar pattern during 2014 as that described above; gradual warming during spring, followed by cooling as summertime upwelling occurred, followed by very rapid warming between August and September. This rapid warming in the fall was due to an advection of the blob waters into the coastal region, which is particularly apparent in the buoy data for locations between 34°N and 45°N (fig. 40, right-hand panels). For those stations, the increase in temperatures from slightly above the climatological mean to greater than 2 standard deviations above the mean occurred in as little as a week, or even within 1 day, as was observed off Stonewall Bank. Although this is a typical process whereby upwelling shuts down and warm waters advect onshore, the difference in 2014 was that the waters

moving onshore were several degrees above the typical temperatures seen within the coastal CCS upon the cessation of upwelling. Although the blob was located more towards the northern CCS and centered near the Gulf of Alaska, warming in the nearshore regions sampled by the buoys actually began progressively earlier in the southern stations, particularly as compared to Stonewall Bank. The most likely reason for this is that upwelling was still active in the northern areas through mid-September, whereas upwelling in the south had decreased dramatically (negative anomaly) as early as July (fig. 2).

Summarizing, warming in the surface waters proceeded as follows: 1) waters within the Gulf of Alaska warmed during the fall of 2013 due to changes in atmospheric forcing, 2) waters offshore of Oregon, California, and within the Southern California Bight warmed gradually during spring 2014, also likely due to changes in atmospheric forcing, 3) coastal warming decreased during summer 2014, due to low, but still effective, coastal upwelling, 4) with the cessation of upwelling in the fall of 2014 (Aug–Sept) waters in the nearshore saw dramatic advective-related warming as the offshore anomalies moved into the coast, starting in the south first, and 5) waters in both offshore and nearshore remained anomalously warm through the winter of 2014–early spring 2015, until upwelling began in April–May of 2015. After the cessation of upwelling in summer/fall 2015, most stations then show a pattern of warming very similar to that seen during the fall of 1997 (fig. 40), suggesting that the CCS may finally be responding to the impacts of El Niño.

Ecosystem Response Overview

The productivity of the system during 2014, as observed by the standing stock of chlorophyll *a* (a proxy for system productivity), was reduced compared to 2013. The low productivity was a result of weak upwelling during the summer of 2014 and extremely low mixed layer concentrations of nitrate, or a nutrient co-varying with it, as seen throughout the CalCOFI domain. Low nutrient concentrations within the mixed layer, in turn, were a consequence of deep nitraclines (fig. 12). 2015 saw an increase in upwelling within the northern regions of the CCS relative to 2014, resulting in more phytoplankton standing stock than the previous year, however, it was spatially and temporally patchy.

Every contribution to this report that included samples for species abundance and composition during 2015 saw drastic changes from previous sampling. Off Washington and Oregon, high abundances of anchovy and sardine larvae were found, along with fish that had very rarely if ever been identified within those trawls. Similarly, off Oregon, the copepod assemblage was augmented by rare or previously unrecorded species, thought to consist mainly of warm-water offshore species (B. Peterson, pers com), along with both "northern" and high abundances of "southern" affiliated copepods, leading to high species richness. The appearance of these rare, presumably warm-water offshore species is critical, as it further supports the hypothesis that source waters were from far offshore, likely due to advection of blob waters. High abundances of jellies were also found off coastal Oregon (particularly *Aequorea* spp.), whereas high abundances of tunicates were found off the more central region of the coastal CCS. Although juvenile rockfish abundances remained high along the central coast, the abundance of euphausiids, squid, and sanddab decreased throughout much of the central CCS. Very few, if any sardine or anchovy were found off southern California, although significant numbers of dorado eggs were found (something that has rarely occurred, except during extreme warm water events). The two community analyses that were conducted both showed 2015 as an extreme outlier compared to all other years, including the 1997–98 El Niño, although in the central CCS trawls, species were found which are typically associated with strong El Niños. These same samples also contained relatively high abundances of coastal upwelling-related species, along with warm-water offshore affiliated species. The presence of these three different groups that come from different water masses within the same samples suggests 2015 may have had one of the sharpest gradients in onshore to offshore temperatures (and thus also water masses) as possibly any other recorded time, given the offshore temperatures reaching up to 4°C above the climatological mean, while at the same time, significant coastal upwelling occurred along the central and northern coast.

Unlike fish and invertebrates, seabirds and marine mammals had mixed responses during 2014 (2015 data for some of these species is yet to be processed), presumably depending on their abilities to compensate for changes in their normal prey, and depending on their location relative to the patchiness in upwelling and productivity. Murres off Yaquina Head, Oregon had decreased success during 2014 as compared to 2013, whereas the murres and Brandt's cormorants at Castle Rock, CA, showed average or increased productivity. Similarly, the seabirds on southeast Farallon Island showed both species with higher and lower breeding success during 2014. Seabirds within the CalCOFI domain had average species richness during 2014–15, and an increase in the presence of sooty shearwaters and Cook's petrel during the spring-time cruises in both 2014 and 2015. For sea lions, 2014 saw decreased weights and growth rates for the pups, and 2015 is expected to be an extremely poor year for them due to changes in their feeding environment.

Summary

The common theme for the California Current system during 2014–15 is the dramatic change from the previous year, in both physical and biological properties. The intrusion of the offshore anomalously warm waters (e.g., the blob) brought both "new" warm-water offshore species, and also typically El Niño-related species into or within near proximity of the nearshore coastal regions. Unlike the lead-in to past strong El Niño's, 2015 still saw considerable amounts of effective upwelling in the central and northern regions, thus coastal, upwelling-related species (such as rockfish juveniles) were still found in relatively high abundances. The result is a system with overall moderate productivity (depending on location), extremely high species diversity, and overall changes in ecosystem structure. Although not documented in the sampling presented here, during 2015 there was also an unprecedented harmful algal bloom, primarily of the genus *Pseudo-nitzchia* sp., which produces the toxin domoic acid. This bloom ranged form Alaska to southern California by July, and resulted in the closure of many fisheries along the US West Coast (for further details, see: http://www.nwfsc.noaa.gov/news/features/west_coast_algal_bloom/index.cfm). The question now remains as to how long these conditions will persist; has the CCS transitioned to yet a new state or phase in a cycle that is different from previously observed cycles, or are we seeing merely a transitional period? Given what is known of past El Niños and atmospheric teleconnections (Schwing et al. 2008), one possible scenario is that as the El Niño begins to more heavily influence the region, it will alter the atmospheric patterns that created the blob and thus return the system to a more typical warm-phase PDO condition, with the overlaid El Niño forcing (N. Mantua pers com). Whether the ecosystem will also return to a relatively similar "known" state, will remain to be observed.

ACKNOWLEDGEMENTS

Andrew W. Leising was partially funded through NOAA's Fisheries and the Environment (FATE) program. Ichthyoplankton collections off the Oregon coast were supported in part by NOAA's Stock Assessment Improvement Plan (SAIP) and Fisheries and the Environment (FATE) programs, as well as from a grant through the Bonneville Power Administration (BPA). Observations along the Trinidad Head Line were also supported in part by NOAA's SAIP and FATE programs, the able assistance of crew from HSU's RV *Coral Sea*, numerous HSU students, and research assistants. Financial support was provided by the NASA Ocean Biology and Biogeochemistry Program Grants NNX09AT01G (M.K.), National Science Foundation (Grant OCE-1026607 to the CCE LTER program). Satellite data were provided by the NASA Ocean Color Processing Group and ESA MERIS team. We thank the CalCOFI and CCE-LTER programs, NOAA SWFSC survey, Monterey Bay Aquarium Research Institute, and Pacific Coastal Ocean Observing System for in situ data. R. DeLong, J. Harris, H. Huber, J. Laake, A. Orr, and many field assistants participated in the data collection and summaries. Funding was provided by the National Marine Fisheries Service. Research was conducted under NMFS Permit 16087 issued to the National Marine Mammal Laboratory. The IMECOCAL program thanks students, technicians, researchers, and crew of the CICESE RV *Francisco de Ulloa* and INAPESCA RV *BIPO* who participated in the surveys. IMECOCAL surveys were supported by CICESE, SEMARNAT-CONACYT 107267, and SEP-CONACYT 129140 and 129611 projects. The summer 2004 survey was in collaboration with INAPESCA-SAGARPA and CICIMAR-IPN. Thanks to Erasmo Miranda for processing CTD data, and to Martin De la Cruz for chlorophyll *a* analyses.

LITERATURE CITED

Auth, T. D. 2011. Analysis of the spring–fall epipelagic ichthyoplankton community in the northern California Current in 2004–09 and its relation to environmental factors. Calif. Coop. Oceanic. Fish. Invest. Rep. 52:148–167.

Bakun, A. 1973. Coastal upwelling indices, west coast of North America, 1946–71. U.S. Dep. Commer., NOAA Tech. Rep., NMFS SSRF-671, 103 p.

Bjorkstedt, E., R. Goericke, S. McClatchie, E. Weber, W. Watson, N. Lo, B. Peterson, B. Emmett, R. Brodeur, J. Peterson, M. Litz, J. Gomez-Valdez, G. Gaxiola-Castro, B. Lavaniegos, F. Chavez, C. A. Collins, J. Field, K. Sakuma, P. Warzybok, R. Bradley, J. Jahncke, S. Bograd, F. Schwing, G. S. Campbell, J. Hildebrand, W. Sydeman, S. Thompson, J. Largier, C. Halle, S. Y. Kim, and J. Abell. 2012. State of the California Current 2010–11: Regional Variable Responses to a Strong (But Fleeting?) La Niña. California Cooperative Oceanic Fisheries Investigations Report 52:36–68.

Bograd, S. J., I. Schroeder, N. Sarkar, X. M. Qiu, W. J. Sydeman, and F. B. Schwing. 2009. Phenology of coastal upwelling in the California Current. Geophysical Research Letters 36:doi 10.1029/2008gl035933.

Bograd, S. J., M. P. Buil, E. Di Lorenzo, C. G. Castro, I. D. Schroeder, R. Goericke, C. R. Anderson, C. Benitez-Nelson, F. A. Whitney. Changes in source waters to the Southern California Bight, Deep Sea Research Part II: Topical Studies in Oceanography, Volume 112, February 2015, Pages 42–52, ISSN 0967–0645, http://dx.doi.org/10.1016/j.dsr2.2014.04.009.

Bond, N. A., M. F. Cronin, H. Freeland, and N. Mantua. 2015. Causes and impacts of the 2014 warm anomaly in the NE Pacific. Geophys. Res. Lett., 42, 3414–3420. doi: 10.1002/2015GL063306.

Brodeur, R. D., J. P. Fisher, R. L. Emmett, C. A. Morgan, and E. Casillas. 2005. Species composition and community structure of pelagic nekton off Oregon and Washington under variable oceanographic conditions. Mar. Ecol. Prog. Ser. 298: 41–57.

Daly, E. A., T. D. Auth, R. D. Brodeur, and W. T. Peterson. 2013. Winter ichthyoplankton biomass as a predictor of early summer prey fields and survival of juvenile salmon. Mar. Ecol. Prog. Ser. doi:10.3359/meps10320.

Di Lorenzo, E., N. Schneider, K. M. Cobb, P. J. S. Franks, K. Chhak, A. J. Miller, J. C. McWilliams, S. J. Bograd, H. Arango, E. Curchitser, T. M. Powell, and P. Riviere. 2008. North Pacific Gyre Oscillation links ocean climate and ecosystem change. Geophysical Research Letters 35:doi 10.1029/2007gl032838.

Durazo, R., and T. Baumgartner. 2002. Evolution of oceanographic conditions off Baja California: 1997–99. *Progr. Oceanogr.*, 54, 7–31.

Durazo, R. 2015. Seasonality of the transitional region of the California Current System off Baja California. *Journal of Geophysical Research-Oceans,* 120, 1173–1196, doi:10.1002/2014JC010405.

Gladics, A. J., R. M. Suryan, R. D. Brodeur, L. M. Segui, and L. Z. Filliger. 2014. Constancy and change in marine predator diets across a shift in oceanographic conditions in the Northern California Current. Marine Biology 161:837–851.

Gladics, A. J., R. M. Suryan, J. K. Parrish, C. A. Horton, E. A. Daly, and W. T. Peterson. 2015. Environmental drivers and reproductive consequences of variation in the diet of a marine predator. Journal of Marine Systems 146:72–81.

Hayward, T. L. 2000. El Niño 1997–98 in the coastal waters of Southern California: A timeline of events. CalCOFI Reports 41, 98–116.

Hoton, C. A. 2014. Top-down influences of Bald Eagles on Common Murre populations in Oregon. MS thesis, Oregon State University.

Horton, C. A., and R. M. Suryan. 2012. Brown Pelicans: A new disturbance source to breeding Common Murres in Oregon? Oregon Birds 38:84–88.

Hu, S., A. V. Fedorov, M. Lengaigne, and E. Guilyardi. 2014. The impact of westerly wind bursts on the diversity and predictability of El Niño events: An ocean energetics perspective, Geophys. Res. Lett.,41, 4654–4663, doi:10.1002/2014GL059573.

Hyrenbach, K. D., and R. R. Veit. 2003. Ocean warming and seabird communities of the Southern California Current System (1987–98): response at multiple temporal scales. Deep-Sea Research Part II 50:2537–2565.

Kruskal, J. B. 1964. Nonmetric multidimensional scaling: a numerical method. Psychometrika 29: 115–130.

Leising, A. W., et al. 2014. State of the California Current 2013–14: El Niño looming. California Cooperative Ocean and Fisheries Investigations Reports 55:31–87.

Ljung, L. System Identification: Theory for the User, Upper Saddle River, NJ, Prentice-Hal PTR, 1999.

Ludescher, J., A. Gozolchiani, M. I. Bogachev, A. Bunde, S. Havlin, and H. J. Schellnhuber. 2014. Very early warning of next El Niño. Proceedings of the National Academy of Sciences 111:2064–2066.

Lynn, R. J., and S. J. Bograd. 2002. Dynamic Evolution of the 1997–99 El Niño-La Niña cycle in the southern California Current system. Prog. Oceanogr. 54.

Lynn, R. J., and J. J. Simpson. 1987. The California Current system: The seasonal variability of its physical characteristics. *J. Geophys. Res.*, 92, 12,947–12,966.

Mantua, N. J., S. R. Hare, Y. Zhang, J. M. Wallace, and R. C. Francis. 1997. A Pacific Interdecadal Climate Oscillation with Impacts on Salmon Production. Bulletin of the American Meteorological Society 78:1069–1079.

Melin, S. R., A. J. Orr, J. D. Harris, J. L. Laake, R. L. DeLong, F. M. D. Gulland, and S. Stoudt. 2010. Unprecedented mortality of California sea lion pups associated with anomalous oceanographic conditions along the central California coast in 2009. California Cooperative Ocean and Fisheries Investigations Reports 51: 182–194.

Melin, S. R., A. J. Orr, J. D. Harris, J. L. Laake, and R. L. DeLong. 2012. California sea lions: An indicator for integrated ecosystem assessment of the California Current System. California Cooperative Ocean and Fisheries Investigations Reports 53:140–152.

Ohman, M., and E. Venrick. 2003. CalCOFI in a changing ocean. Oceanography 16, 76–85.

Perrins, C. M. 1970. The timing of birds' breeding seasons. Ibis 112: 242–255.

Ralston, S., and I. J. Stewart. 2013. Anomalous distributions of pelagic juvenile rockfish on the U.S. west coast in 2005 and 2006. CalCOFI Reports 54:155–166.

Ralston, S., K. M. Sakuma, and J. C. Field. 2013. Interannual variation in pelagic juvenile rockfish (*Sebastes* spp.) abundance—going with the flow. Fisheries Oceanography 22:4: 288–308.

Ralston, S., J. C. Field, and K. M. Sakuma. 2015. Longterm variation in a central California pelagic forage assemblage. Journal of Marine Systems (in press). http://dx.doi.org/10.1016/j.jmarsys.2014.06.013.

Reed, T. E., S. Waneless, M. P. Harris, M. Frederiksen, L. E. B. Kruuk, and E. J. A. Cunningham. 2006. Responding to environmental change: plastic responses vary little in a synchronous breeder. Proceedings of the Royal Society of London B 273:2713–2719.

Santora, J. A., I. D. Schroeder, J. C. Field, B. K. Wells, and W. J. Sydeman. 2014. Spatio-temporal dynamics of ocean conditions and forage taxa reveals regional structuring of seabird-prey relationships. Ecological Applications Ecological Applications 24:7:1730–1747.

Santora, J. A., and W. J. Sydeman. 2015. Persistence of hotspots and variability of seabird species richness and abundance in the southern California Current. Ecosphere, *in press*.

Schroeder, I. D., W. J. Sydeman, N. Sarkar, S. A. Thompson, S. J. Bograd, and F. B. Schwing. 2009. Winter pre-conditioning of seabird phenology in the California Current.

Schwing, F. B., M. O'Farrell, J. M. Steger, and K. Baltz. 1996. Coastal upwelling indices, West Coast of North America, 1946–1995, NOAA Tech. Memo., NOAA-TMNMFS-SWFSC-231, 144 pp.

Schwing, F. B., R. Mendelssohn, S. J. Bograd, J. E. Overland, M. Wang, S. Ito. Climate change, teleconnection patterns, and regional processes forcing marine populations in the Pacific, Journal of Marine Systems, Volume 79, Issues 3–4, 10 February 2010, Pages 245–257, ISSN 0924-7963, http://dx.doi.org/10.1016/j.jmarsys.2008.11.027.

Suchman, C. L., R. D. Brodeur, E. A. Daly, and R. L. Emmett. 2012. Large medusae in surface waters of the Northern California Current: variability in relation to environmental conditions. *Hydrobiologia*. 690:113–125.

Sydeman, W. J., K. L. Mills, J. A. Santora, S. A. Thompson, D. F. Bertram, K. H. Morgan, B. K. Wells, J. M. Hipfner, and S. G. Wolf. 2009. Seabirds and climate in the California Current—A synthesis of change. CalCOFI Report 50:82–104.

Sydeman, W. J., S. A. Thompson, J. A. Santora, J. A. Koslow, R., Goericke, and M. D. Ohman. 2015. Climate-ecosystem change off southern California: time-dependent seabird predator-prey numerical responses. Deep-Sea Research Part II:158–170.

Veit, R. R., P. Pyle, and J. A. McGowan. 1996. Ocean warming and long-term change in pelagic bird abundance within the California Current system. Marine Ecology Progress Series 139:11–18.

Wells, B. K., and 47 other authors. 2013. State of the California Current 2012–13: No such thing as an "average" year. CalCOFI Reports 54: 37–71.

Wolter, K. and M. S. Timlin. 1998. Measuring the strength of ENSO events—how does 1997/98 rank? Weather 53:315–324.

Yen, P. P. W., W. J. Sydeman, S. J. Bograd, and K. D. Hyrenbach. 2006. Spring-time distributions of migratory marine birds in the southern California Current: oceanic eddy associations and coastal habitat hotspots over 17 years. Deep-Sea Research II 53: 399–418.